AD-A034 914 TEXAS UNIV AT AUSTIN ELECTRONICS RESEARCH CENTER F/G 9/4
THE DESIGN OF MULTIDIMENSIONAL FIR DIGITAL FILTERS BY PHASE COR--ETC(U)
AUG 76 M T MANRY, J K AGGARWAL F44620-76-C-0089
UNCLASSIFIED TR-181 AFOSR-TR-77-0008 NL

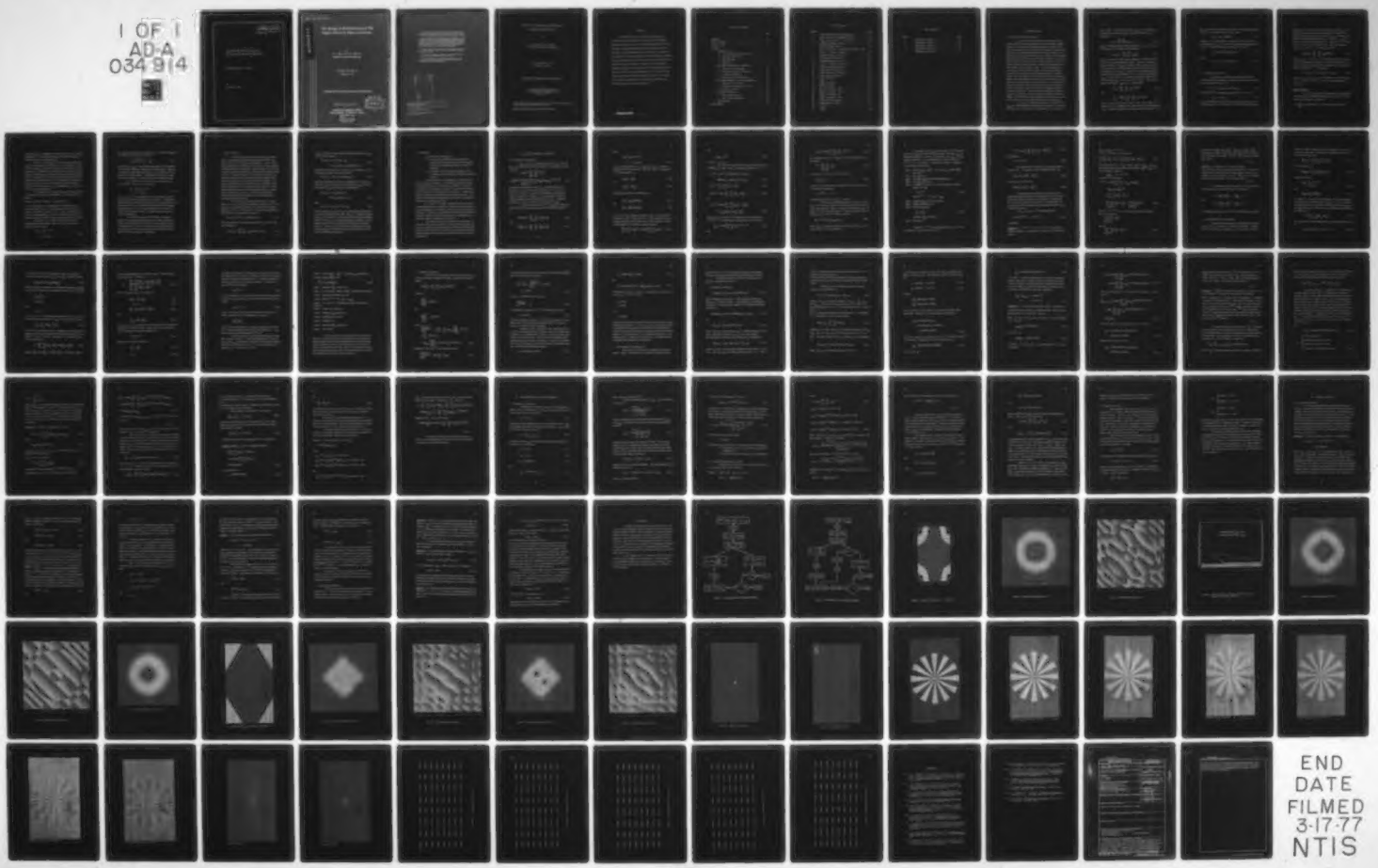

END
DATE
FILMED
3-17-77
NTIS

THE DESIGN OF MULTIDIMENSIONAL FIR DIGITAL FILTERS BY PHASE CORRECTION

TEXAS UNIVERSITY AT AUSTIN

12 AUGUST 1976

The Design of Multidimensional FIR Digital Filters by Phase Correction

by

M. T. Manry and J. K. Aggarwal

Department of Electrical Engineering

Technical Report No. 181

August 12, 1976

INFORMATION SYSTEMS RESEARCH LABORATORY

Approved for public release;
distribution unlimited.

ELECTRONICS RESEARCH CENTER
THE UNIVERSITY OF TEXAS AT AUSTIN
Austin, Texas 78712

The Electronics Research Center at The University of Texas at Austin constitutes interdisciplinary laboratories in which graduate faculty members and graduate candidates from numerous academic disciplines conduct research.

Research conducted for this technical report was supported in part by the Department of Defense's JOINT SERVICES ELECTRONICS PROGRAM (U.S. Army, U.S. Navy, and the U.S. Air Force) through the Research Contract AFOSR F44620-71-C-0091. This program is monitored by the Department of Defense's JSEP Technical Advisory Committee consisting of representatives from the U.S. Army Electronics Command, U.S. Army Research Office, Office of Naval Research, and the U.S. Air Force Office of Scientific Research.

Additional support of specific projects by other Federal Agencies, Foundations, and The University of Texas at Austin is acknowledged in footnotes to the appropriate sections.

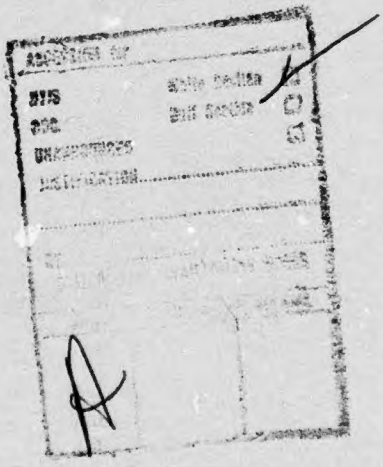

THE DESIGN OF MULTIDIMENSIONAL FIR DIGITAL FILTERS BY PHASE CORRECTION *

by

M. T. Manry and J. K. Aggarwal
Department of Electrical Engineering

Technical Report No. 181
August 12, 1976

INFORMATION SYSTEMS RESEARCH LABORATORY

ELECTRONICS RESEARCH CENTER
THE UNIVERSITY OF TEXAS AT AUSTIN
Austin, Texas 78712

*This research was supported in part by the Joint Services Electronics Program under Contract F44620-76-C-0089.

ABSTRACT

This report presents a new technique for the design of multidimensional FIR digital filters. Given the desired amplitude response, the truncation error of a low order approximation to a high order filter is iteratively decreased by varying the phase response. Convergence of the iterative algorithm is discussed. In general, the phase responses of the filters resulting from the algorithm are nonlinear. Pictures suffer phase distortion when filters with nonlinear phase characteristics are used in filtering. A measure of phase distortion in pictures is introduced so that the effects of nonlinear phase in filters may be quantified. Examples illustrating the use of the design technique and the measure of phase distortion are included. The results of this report are formulated in two dimensions; however they are valid for filters and signals of any dimension.

TABLE OF CONTENTS

LIST OF FIGURES

LIST OF TABLES

I. INTRODUCTION

A. Two-Dimensional Digital Filtering

In the last several years digital techniques have found widespread use in image processing due to the availability of digital computers, the large number of operations which computers can perform, the increasing speed at which these operations can be performed, and the advent of efficient algorithms for carrying out certain processing tasks. The operation most widely used in digital image processing is the linear operation known as convolution or filtering. In [1], Rindfleisch, Dunne, Frieden, Stromberg, and Ruiz describe the use of convolution and other digital processing techniques for the enhancement of the Mariner 6 and 7 pictures of Mars. Many degradations of pictures, such as motion and defocus blurs, may be described as the convolution of an ideal picture with a degrading signal. Stockham, Cannon, and Ingebretsen [2] have shown how to identify the degrading signal, when it is not known, and how to remove it through a second convolution, which is known as a deconvolution. Lewis and Sakrison [3] have used Wiener filters to reduce noise and optical distortion in electron micrographs. Duda and Hart [4] have suggested filtering as an aid to scene analysis. They have shown the effects, on pictures, of low pass, high pass, and high emphasis two-dimensional digital filtering. In the oil industry two dimensional digital filtering is being used to remove multiple reverberations from marine seismic data.

Let $\{f_{mn}\}$ be a digital input sequence or picture and let $\{h_{mn}\}$ be a two-dimensional impulse response sequence. We assume that $\{h_{mn}\}$ has M rows and N columns and that $\{f_{mn}\}$ is the same

size or larger. When the input sequence $\{f_{mn}\}$ is convolved with or filtered by the sequence $\{h_{mn}\}$, the output picture $\{\tilde{p}_{mn}\}$ is described by

$$\tilde{p}_{mn} = \sum_{k=0}^{M-1} \sum_{\ell=0}^{N-1} h_{k\ell} f_{m-k,n-\ell} \quad . \tag{1.1}$$

The two-dimensional digital filter represented by $\{h_{mn}\}$ may also be described by the Z-transform transfer function,

$$Ha(Z_1,Z_2) = \sum_{m=0}^{M-1} \sum_{n=0}^{N-1} h_{mn} Z_1^m Z_2^n \quad . \tag{1.2}$$

$Ha(Z_1,Z_2)$ is called a finite impulse response or FIR digital filter if M and N are finite nonnegative integers. If M or N are infinite positive integers, $Ha(Z_1,Z_2)$ is called an infinite impulse response or IIR digital filter. The frequency response of the filter $Ha(Z_1,Z_2)$ is $Ha(\exp(-j\omega_1), \exp(-j\omega_2))$, which may be evaluated through use of the discrete Fourier transform or DFT. For every spatial sequence $\{h_{mn}\}$ of length (M,N), we can find a corresponding frequency domain sequence $\{H_{k\ell}\}$, which is the DFT of $\{h_{mn}\}$. The DFT relationship, denoted as $h_{mn} \leftrightarrow H_{k\ell}$, is described as

$$H_{k\ell} = \sum_{m=0}^{M-1} \sum_{n=0}^{N-1} h_{mn} U^{km} V^{\ell n} \tag{1.3}$$

and

$$h_{mn} = (1/MN) \sum_{k=0}^{M-1} \sum_{\ell=0}^{N-1} H_{k\ell} U^{-km} V^{-\ell n}, \tag{1.4}$$

where $U = \exp(-j\,2\pi/M)$ and $V = \exp(-j\,2\pi/N)$. Thus a filter described by (1.2) is specified by the MN points of the spatial sequence, $\{h_{mn}\}$, or by the MN points of the frequency domain sequence, $\{H_{k\ell}\}$.

The frequency domain sequence is expressed by an amplitude sequence, $\{|H_{k\ell}|\}$, and a phase sequence, $\{\theta_{k\ell}\}$, where

$$H_{k\ell} = |H_{k\ell}| \exp(j\theta_{k\ell}). \tag{1.5}$$

In general, for a given amplitude sequence, distinct choices of the phase sequence $\{\theta_{k\ell}\}$, lead to distinct impulse response sequences, $\{h_{mn}\}$. The relationship between $Ha(Z_1, Z_2)$ and $\{H_{k\ell}\}$ is

$$H_{k\ell} = Ha(\exp(-j\omega_1), \exp(-j\omega_2)) \tag{1.6}$$

where

$$(\omega_1, \omega_2) = ((2\pi/M)k, (2\pi/N)\ell) \ . \tag{1.7}$$

B. FIR Digital Filter Design

In designing a two-dimensional digital filter we are usually given a desired frequency response which may be expressed, using amplitude and phase, as

$$H(\omega_1, \omega_2) = |H(\omega_1, \omega_2)| \exp(j\theta^d(\omega_1, \omega_2)) \ . \tag{1.8}$$

One may design an FIR digital filter using (1.4), (1.7), and

$$H_{k\ell} = H(\omega_1, \omega_2) \ . \tag{1.9}$$

The resulting filter $Ha(Z_1, Z_2)$ has the desired frequency response at the MN points of (1.7). However, if M and N are large enough for

$Ha(\exp(-j\omega_1), \exp(-j\omega_2))$ to closely approximate $H(\omega_1,\omega_2)$, then $Ha(Z_1,Z_2)$ usually has too many coefficients to be useful. This problem is attacked by designing a filter $\hat{Ha}(Z_1,Z_2)$, with few coefficients, which approximates $Ha(Z_1,Z_2)$ or $H(\omega_1,\omega_2)$. Let T_0 be the set of nonnegative integer pairs (m,n), where $0 \le m \le M-1$ and $0 \le n \le N-1$, and let T be a subset of T_0. Given the spatial sequence $\{h_{mn}\}$, $(m,n) \in T_0$, we wish to form a filter

$$\hat{Ha}(Z_1,Z_2) = \sum_{m=0}^{M-1} \sum_{n=0}^{N-1} \hat{h}_{mn} Z_1^m Z_2^n , \tag{1.10}$$

such that $\hat{h}_{mn} = 0$ if $(m,n) \notin T$. The other coefficients are chosen so that the approximation is accurate. In general T may be any set of nonnegative integer pairs satisfying the condition above, however in this report the choice of T is restricted to

$$T = \{(m,n) \in Z^2 \mid 0 \le m \le M_1, \; 0 \le n \le N_1\}, \tag{1.11}$$

where $M_1 < M-1$, $N_1 < N-1$, and Z^2 denotes the set of all integer pairs. In this case $\hat{Ha}(Z_1,Z_2)$ is a low order approximation of $Ha(Z_1,Z_2)$.

Design Techniques

Recently minimax methods for designing two-dimensional FIR filters have been explored by Hersey and Mersereau [5]. Their technique minimizes the error function

$$E_m = \max_{\omega_1,\omega_2} \left| W(\omega_1,\omega_2)\left(|H(\omega_1,\omega_2)| - |\hat{Ha}(\exp(-j\omega_1),\exp(-j\omega_2))|\right)\right|$$

where $W(\omega_1,\omega_2)$ is a weighting function and $\hat{H}a(Z_1,Z_2)$ is restricted to linear phase. Unfortunately minimax design techniques require a prohibitive amount of computation time.

Another two-dimensional FIR filter design method is the frequency sampling method developed by Hu and Rabiner [6]. When a filter is designed by frequency sampling the DFT frequency domain coefficients, corresponding to pass-bands and stop-bands, are fixed. The error of approximation is minimized with respect to the transition-band DFT coefficients. The impulse response coefficients are then calculated by taking the inverse DFT. An advantage of this filter design method is that it can be used to approximate any frequency response. This method consumes a lot of computation time, but not as much time as a minimax method.

Two-dimensional FIR digital filters may be designed using the transformation approach of McClellan [7]. In this approach the equation

$$\cos(\omega) = A\cos(\omega_1) + B\cos(\omega_2) + C\cos(\omega_1)\cos(\omega_2) + D$$

is used to transform a one-dimensional filter $\hat{H}(\omega)$ into a two-dimensional filter $\hat{H}(\omega_1,\omega_2)$. Different types of filters may be designed by changing the constants A, B, C, and D. This is the fastest of the design techniques. However, the method applies only to linear phase filters and there are severe amplitude constraints as well.

Truncation is the simplest design method for two-dimensional FIR digital filters. Given $Ha(Z_1,Z_2)$ and the set T, $\hat{H}a(Z_1,Z_2)$ is formed using

$$\begin{aligned} \hat{h}_{mn} &= h_{mn}, (m,n)\in T \ , \\ &= 0 \ , (m,n)\notin T \ . \end{aligned} \qquad (1.12)$$

Let $\{\hat{H}_{k\ell}\}$ be the order (M,N) DFT of $\{\hat{h}_{mn}\}$. Truncation minimizes the summation of squares error function,

$$E_\ell = \sum_{k=0}^{M-1} \sum_{\ell=0}^{N-1} |H_{k\ell} - \hat{H}_{k\ell}|^2 \ , \tag{1.13}$$

with respect to $\{\hat{h}_{mn}\}$. This filter design method has the advantage that any desired frequency response may be approximated. There are no amplitude or linear phase constraints. Also, truncation is an extremely fast design technique. Unfortunately the frequency domain error, due to truncation, is usually severe near transition regions.

To lessen the bad effects of truncation, windowing is often employed. When (1.12) is replaced by

$$\begin{aligned} \hat{h}_{mn} &= h_{mn} w_{mn}, (m,n) \in T \ , \\ &= 0 \ , \quad (m,n) \notin T \ , \end{aligned} \tag{1.14}$$

where $\{w_{mn}\}$ is a window sequence, the severe ripples in the frequency response of the truncated filter are smoothed. Huang [8] has demonstrated that two-dimensional windows may be designed from one-dimensional windows. A problem with windowing is that it extends transition regions. This is undesirable when sharp cutoffs are required in the amplitude response. In addition windowing is not an optimal design method.

Of all the two-dimensional FIR digital filter design methods, only truncation and windowing lead to filters, which approximate any desired frequency response, in a reasonable amount of computation time. The field of image processing may be significantly advanced if the truncation design method is improved and the need for windowing is reduced or eliminated.

C. Phase Distortion

It is being increasingly recognized that when complex signals such as Fourier transforms are represented in polar coordinates, phase is more important than amplitude. Larmore, El-Sum, and Metherell [9] and also Kermisch [10] have shown the importance of phase information in holography. Huang, Burnett, and Deczky [11] have demonstrated the significance of phase in digital image processing filters. In general the phase of a digital filter will have error. Linear phase, which does not degrade the phase of input signals, cannot be obtained in causal, realizable IIR digital filters. Even though FIR digital filters may have linear phase, this phase often has discontinuities of π. Nonlinear phase characteristics, which may be specified for Wiener filters and matched filters, are generally not realizable with zero error. The filter design method of Steiglitz [12] minimizes a magnitude error function and leads to nonlinear phase characteristics.

Let $\hat{H}(\omega_1, \omega_2)$ be the frequency response of a digital filter. Let $H(\omega_1, \omega_2)$ be the desired frequency response, as in (1.8). $\hat{H}(\omega_1, \omega_2)$ has amplitude and phase error and may be the frequency response of an IIR or FIR digital filter. The frequency response may be expressed, using amplitude and phase, as

$$\hat{H}(\omega_1, \omega_2) = |\hat{H}(\omega_1, \omega_2)| \exp(j\theta(\omega_1, \omega_2)) \quad . \tag{1.15}$$

The Fourier transform of a digital input picture $\{f_{mn}\}$ with M rows and N columns is

$$F(\omega_1, \omega_2) = \sum_{m=0}^{M-1} \sum_{n=0}^{N-1} f_{mn} \exp(-j(m\omega_1 + n\omega_2)) \quad . \tag{1.16}$$

If $\{f_{mn}\}$ is filtered using the desired filter the output picture $\{p_{mn}\}$ has the Fourier transform

$$P(\omega_1,\omega_2) = F(\omega_1,\omega_2)H(\omega_1,\omega_2)$$
$$= F(\omega_1,\omega_2)|H(\omega_1,\omega_2)|\exp(j\theta^d(\omega_1,\omega_2)) \quad . \tag{1.17}$$

The effects of the phase error of $\hat{H}(\omega_1,\omega_2)$ are of interest to us, so we therefore construct a frequency response

$$\tilde{H}(\omega_1,\omega_2) = |H(\omega_1,\omega_2)|\exp(j\theta(\omega_1,\omega_2)) \quad , \tag{1.18}$$

which has the phase error but not the amplitude error of $\hat{H}(\omega_1,\omega_2)$. When $\tilde{H}(\omega_1,\omega_2)$ is used to filter the input picture $\{f_{mn}\}$, the output picture is $\{\hat{p}_{mn}\}$ which has the Fourier transform

$$\hat{P}(\omega_1,\omega_2) = F(\omega_1,\omega_2)\tilde{H}(\omega_1,\omega_2)$$
$$= P(\omega_1,\omega_2)\exp(jm(\omega_1,\omega_2)) \tag{1.19}$$

where

$$m(\omega_1,\omega_2) = \theta(\omega_1,\omega_2) - \theta^d(\omega_1,\omega_2) \quad . \tag{1.20}$$

The error between $\{p_{mn}\}$ and $\{\hat{p}_{mn}\}$ is called phase distortion and is caused by the phase error function $m(\omega_1,\omega_2)$. The phase response $\theta(\omega_1,\omega_2)$ is acceptable in a given application if the phase distortion produced by $m(\omega_1,\omega_2)$ is measured and found to be small. One may attempt to measure the phase distortion of filtering by measuring $m(\omega_1,\omega_2)$. However, such a measure does not change as the input picture changes. This type of measure has the same value for sine wave and wideband input pictures.

D. Objectives

The objectives of this report are

(1) To develop a two-dimensional FIR digital filter design method which leads to amplitude responses, better than those obtainable through truncation and windowing,

(2) To develop a measure of phase distortion, caused by filtering, for the evaluation of the phase responses of filters.

A design method for two-dimensional FIR digital filters, which we call phase correction, is developed and analyzed in Chapter II of this document. The basic design algorithm is derived and its convergence is discussed in section IIA. In section IIB the algorithm is improved so that convergence is more rapid. A comparison of phase correction to gradient techniques is made in section IIC. The problems of initializing the algorithm and measuring the phase error of the filters are treated in section IID.

In Chapter III a measure of phase distortion in pictures is formulated and its uses are described. The measure of phase distortion is developed from the Euclidean distance between two pictures in section IIIA. Methods of calculating the measure and evaluating phase responses of filters are given in section IIIB. An efficient way to estimate the measure is formulated in section IIIC.

We design several filters in section IVA to illustrate the use of the phase correction algorithm. Filters designed by phase correction are compared to filters designed by truncation and windowing. In section IVB two filters are used to filter a test pattern input picture and the resulting phase distortion in the output pictures is measured and estimated.

II. THE PHASE CORRECTION ALGORITHM

A. Derivation of the Algorithm

Given the desired amplitude sequence $\{|H_{k\ell}|\}$ and the set T, the truncation error between $Ha(Z_1, Z_2)$ and $\hat{Ha}(Z_1, Z_2)$ may be written as

$$I(\{\theta_{k\ell}\}) = \sum_{\substack{m=0 \\ (m,n)\notin T}}^{M-1} \sum_{n=0}^{N-1} |h_{mn}|^2$$

$$= (1/(M^2N^2)) \sum_{\substack{m=0 \\ (m,n)\notin T}}^{M-1} \sum_{n=0}^{N-1} \left| \sum_{k=0}^{M-1} \sum_{\ell=0}^{N-1} |H_{k\ell}| \exp(j\theta_{k\ell}) U^{-km} V^{-\ell n} \right|^2, \qquad (2.1)$$

a function of the phase sequence $\{\theta_{k\ell}\}$. The expression (2.1) is arrived at by the use of the earlier equations (1.2), (1.4), (1.5), and (1.10). $I(\{\theta_{k\ell}\})$ is a measure of the goodness of the approximation of $Ha(Z_1, Z_2)$ by $\hat{Ha}(Z_1, Z_2)$. In this section we derive an iterative method for picking phase sequences, $\{\theta_{k\ell}\}$, so that the error function $I(\{\theta_{k\ell}\})$ is decreased with respect to $\{\theta_{k\ell}\}$.

For the ith iteration, where i is a nonnegative integer, the high order filter and its truncated version are described respectively as

$$Ha^i(Z_1, Z_2) = \sum_{m=0}^{M-1} \sum_{n=0}^{N-1} h_{mn}^i Z_1^m Z_2^n \qquad (2.2)$$

and

$$\hat{Ha}^i(Z_1, Z_2) = \sum_{m=0}^{M-1} \sum_{n=0}^{N-1} \hat{h}_{mn}^i Z_1^m Z_2^n \qquad (2.3)$$

where

$$\hat{h}^i_{mn} = h^i_{mn}, \ (m,n) \in T,$$

$$= 0 \quad , \ (m,n) \notin T. \tag{2.4}$$

It may be emphasized that i is a superscript and not an exponent. The frequency domain sequences, $\{H^i_{k\ell}\}$ and $\{\hat{H}^i_{k\ell}\}$, are obtained from spatial sequences as

$$h^i_{mn} \longleftrightarrow H^i_{k\ell} \tag{2.5}$$

and

$$\hat{h}^i_{mn} \longleftrightarrow \hat{H}^i_{k\ell} \ . \tag{2.6}$$

The amplitude and phase relationships are

$$H^i_{k\ell} = |H_{k\ell}| \exp(j\theta^i_{k\ell}) \tag{2.7}$$

and

$$\hat{H}^i_{k\ell} = |\hat{H}^i_{k\ell}| \exp(j\hat{\theta}^i_{k\ell}). \tag{2.8}$$

As seen in (2.7) the amplitude sequences $\{|H^i_{k\ell}|\}$ are restricted by the equation $|H^i_{k\ell}| = |H_{k\ell}|$ for every i, which implies that the amplitude sequence is held to be the same for every iteration. Further, a simple application of Parseval's equation leads to

$$\sum_{m=0}^{M-1} \sum_{n=0}^{N-1} (h^i_{mn})^2 = (1/MN) \sum_{k=0}^{M-1} \sum_{\ell=0}^{N-1} |H_{k\ell}|^2 = E \tag{2.9}$$

and

$$|h^i_{mn}| \le E^{\frac{i}{2}} \tag{2.10}$$

for every i, m, and n.

Four equivalent expressions for the error between $H\hat{a}^i(Z_1, Z_2)$ and $\hat{H}\hat{a}^p(Z_1, Z_2)$, where i and p are nonnegative integers, are:

$$\text{(i)} \quad I^{ip} = (1/4\pi^2) \int_{-\pi}^{\pi}\int_{-\pi}^{\pi} \left| H\hat{a}^i(\exp(-j\omega_1), \exp(-j\omega_2)) - \hat{H}\hat{a}^i(\exp(-j\omega_1), \exp(-j\omega_2)) \right|^2 d\omega_1\, d\omega_2, \tag{2.11}$$

$$\text{(ii)} \quad I^{ip} = \sum_{m=0}^{M-1}\sum_{n=0}^{N-1} (h^i_{mn} - \hat{h}^p_{mn})^2, \tag{2.12}$$

$$\text{(iii)} \quad I^{ip} = (1/MN) \sum_{k=0}^{M-1}\sum_{\ell=0}^{N-1} |H^i_{k\ell} - \hat{H}^p_{k\ell}|^2, \tag{2.13}$$

and

$$\text{(iv)} \quad I^{ip} = (1/MN) \sum_{k=0}^{M-1}\sum_{\ell=0}^{N-1} |H_{k\ell}|^2 + |\hat{H}^p_{k\ell}|^2 - 2\,|H_{k\ell}|\,|\hat{H}^p_{k\ell}| \cos(\theta^i_{k\ell} - \hat{\theta}^p_{k\ell}). \tag{2.14}$$

Expressions (2.12) and (2.14) follow directly from the evaluation of (2.11) and (2.13), respectively. Expression (2.13) follows when

$$h^i_{mn} = (1/MN) \sum_{k=0}^{M-1}\sum_{\ell=0}^{N-1} H^i_{k\ell}\, U^{-km}\, V^{-\ell n} \tag{2.15}$$

and

$$\hat{h}^{p}_{mn} = (1/MN) \sum_{k=0}^{M-1} \sum_{\ell=0}^{N-1} \hat{H}^{p}_{k\ell}\, U^{-km}\, V^{-\ell n} \tag{2.16}$$

are substituted into (2.12). Using (2.4) in (2.12) and letting $p = i$, we find that

$$I^{ii} = \sum_{\substack{m=0 \\ (m,n)\notin T}}^{M-1} \sum_{n=0}^{N-1} (h^{i}_{mn})^{2}\ , \tag{2.17}$$

and using (2.1), (2.5), (2.7), and (2.17), that

$$I(\{\theta^{i}_{k\ell}\}) = I^{ii}. \tag{2.18}$$

From (2.18) it is obvious that an algorithm which iteratively produces a *decreasing error sequence*,

$$P = \{I^{00}, I^{11}, \ldots, I^{ii}, \ldots\},$$

also decreases the function $I(\{\theta_{k\ell}\})$ iteratively.

Given the desired amplitude sequence $\{|H_{k\ell}|\}$ and the set T, the first step of the phase correction algorithm is to choose an initial phase sequence $\{\theta^{0}_{k\ell}\}$. In order for the sequences $\{h^{i}_{mn}\}$ and $\{\hat{h}^{i}_{mn}\}$ to be real, all phase sequences, including the initial phase sequence, must satisfy the symmetry condition,

$$\theta^{i}_{k\ell} = 2\pi\, n^{i}_{k\ell} - \theta^{i}_{[M-k]_M,[N-\ell]_N}, \tag{2.19}$$

where $\{n^{i}_{k\ell}\}$ is an integer sequence, and $[M-k]_M$, $[N-\ell]_N$, are integers modulo M and N respectively.

The numbers I_E and i_{max} are specified, in the algorithm's first step, to provide an exit from the algorithm. The integer i_{max} is the maximum value of i allowed. In other words, only $(i_{max} + 1)$ iterations are allowed. I_E is a nonnegative real number such that if $I^{i-1,i-1} - I^{ii} < I_E$ for some i, the algorithm is halted. The steps of the algorithm are given below.

Step 0: Given $\{|H_{k\ell}|\}$, $\{\theta^0_{k\ell}\}$, T, I_E, and i_{max}, compute $\{H^0_{k\ell}\}$ from (2.7).

Step 1: Set i equal to 0.

Step 2: Calculate $\{h^i_{mn}\}$ using the relationship (2.5).

Step 3: Get $\{\hat{h}^i_{mn}\}$ from (2.4).

Step 4: Calculate I^{ii} using (2.17). It may be noted, from (2.12) and (2.17), that

$$I^{ii} \leq I^{i,i-1}. \tag{2.20}$$

Exit if $I^{i-1,i-1} - I^{ii} < I_E$ or $i = i_{max}$.

Step 5: Compute $\{\hat{\theta}^i_{k\ell}\}$ from (2.6) and (2.8).

Step 6: Increase the index i by 1.

Step 7: Using the equation

$$\theta^i_{k\ell} = \hat{\theta}^{i-1}_{k\ell}, \tag{2.21}$$

calculate $\{H^i_{k\ell}\}$ from (2.7).

Step 8: Go to Step 2.

Whereas $I^{i-1,i-1}$ can be expressed by (2.14), $I^{i,i-1}$ can be expressed, using (2.14) and (2.21), by

$$I^{i,i-1} = (1/MN) \sum_{k=0}^{M-1} \sum_{\ell=0}^{N-1} (|H_{k\ell}| - |\hat{H}_{k\ell}^{i-1}|)^2. \tag{2.22}$$

This means that

$$I^{i,i-1} \leq I^{i-1,i-1}. \tag{2.23}$$

The implementation of the phase correction algorithm is shown in Fig. 1. In the figure we have implemented Step 7 with

$$H_{k\ell}^{i} = |H_{k\ell}| \, (\hat{H}_{k\ell}^{i-1} / |\hat{H}_{k\ell}^{i-1}|) \tag{2.24}$$

which follows from (2.8), since

$$\exp(j\hat{\theta}_{k\ell}^{i-1}) = \hat{H}_{k\ell}^{i-1} / |\hat{H}_{k\ell}^{i-1}|. \tag{2.25}$$

By alternately decreasing the truncation error in the spatial and frequency domains, the algorithm generates new spatial and frequency domain sequences for each iteration. Inequalities (2.20) and (2.23) imply that the sequence P is nonincreasing, so we have shown that the phase correction algorithm decreases $I(\{\theta_{k\ell}\})$ or leaves it the same.

If $i_{max} = \infty$ and $I_E = 0$ the infinite sequence

$$W = \{I^{00}, I^{10}, I^{11}, \ldots, I^{ii}, I^{i+1,i}, \ldots\} \tag{2.26}$$

is generated.

THEOREM 1: If $I^{ii} = I^{i+1,i}$ or $I^{i+1,i} = I^{i+1,i+1}$ for some finite nonegative integer i, the sequence W converges in a finite number of terms.

PROOF: Case 1 $I^{ii} = I^{i+1,i}$.

By using (2.13) and (2.22) one obtains

$$\sum_{k=0}^{M-1}\sum_{\ell=0}^{N-1} |H_{k\ell}^{i} - \hat{H}_{k\ell}^{i}|^2 = \sum_{k=0}^{M-1}\sum_{\ell=0}^{N-1} (|H_{k\ell}| - |\hat{H}_{k\ell}^{i}|)^2. \tag{2.27}$$

This implies that $\{\theta_{k\ell}^{i}\} = \{\hat{\theta}_{k\ell}^{i}\}$ and that $\{\theta_{k\ell}^{i+1}\} = \{\theta_{k\ell}^{i}\}$. Since the same operations are performed in each iteration, $\{\theta_{k\ell}^{i+p}\} = \{\theta_{k\ell}^{i}\}$ for every nonnegative integer p.

Case 2 $I^{i+1,i} = I^{i+1,i+1}$.

By using (2.22) one obtains

$$\begin{aligned} I^{i+1,i} &= (1/MN) \sum_{k=0}^{M-1}\sum_{\ell=0}^{N-1} \Big| |H_{k\ell}| \exp(j\theta_{k\ell}^{i+1}) \\ &\quad - |\hat{H}_{k\ell}^{i}| \exp(j\theta_{k\ell}^{i+1}) \Big|^2 \\ &= \sum_{m=0}^{M-1}\sum_{n=0}^{N-1} (h_{mn}^{i+1} - \hat{h}_{mn}^{i})^2 \\ &= \sum_{\substack{m=0 \\ (m,n)\in T}}^{M-1}\sum_{n=0}^{N-1} (h_{mn}^{i+1} - \hat{h}_{mn}^{i})^2 + \sum_{\substack{m=0 \\ (m,n)\notin T}}^{M-1}\sum_{n=0}^{N-1} (h_{mn}^{i+1})^2. \end{aligned} \tag{2.28}$$

Now $I^{i+1,i} = I^{i+1,i+1}$, (2.17) and (2.28) imply that the right hand side of (2.28) equals

$$\sum_{\substack{m=0 \\ (m,n)\notin T}}^{M-1}\sum_{n=0}^{N-1} (h_{mn}^{i+1})^2$$

and that

$$\sum_{\substack{m=0 \\ (m,n)\in T}}^{M-1}\sum_{n=0}^{N-1} (h_{mn}^{i+1} - \hat{h}_{mn}^{i})^2 = 0. \tag{2.29}$$

Equation (2.29) implies that $\{\hat{h}^{i+1}_{mn}\} = \{\hat{h}^{i}_{mn}\}$ and $\{\hat{\theta}^{i+1}_{k\ell}\} = \{\hat{\theta}^{i}_{k\ell}\}$, which leads to $\{\theta^{i+2}_{k\ell}\} = \{\theta^{i+1}_{k\ell}\}$. The same operations are carried out for each iteration and therefore $\{\theta^{i+1+p}_{k\ell}\} = \{\theta^{i+1}_{k\ell}\}$ for every nonnegative integer p.

Q.E.D.

Corollary: The sequence W is always convergent.

Proof: This is proved for a special case in theorem 1. From [13] all bounded, non-increasing sequences of real numbers converge. The members of W are bounded by 0 and I^{00}, and W is non-increasing as seen in (2.20) and (2.23). The corollary follows.

Q.E.D.

The convergence of the error sequence W is proved above, but this does not imply the convergence of the sequences,

$$X = \{ \{\hat{h}^{0}_{mn}\}, \{\hat{h}^{1}_{mn}\}, \ldots, \{\hat{h}^{i}_{mn}\}, \ldots \}$$

and

$$Y = \{ \{h^{0}_{mn}\}, \{h^{1}_{mn}\}, \ldots, \{h^{i}_{mn}\}, \ldots \}.$$

The convergence properties of X and Y will be discussed in a paper.

B. Increasing the Rate of Convergence

Normally the phase correction algorithm reduces the error function $I(\{\theta_{k\ell}\})$ significantly in the first few iterations. However, there is often room for improvement. In this section a modified

algorithm, which increases the rate of convergence of the error sequence, is presented. In particular, an algorithm that approximates the high order filter

$$\tilde{H}_a^i(Z_1,Z_2) = \sum_{m=0}^{M-1}\sum_{n=0}^{N-1} \tilde{h}_{mn}^i Z_1^m Z_2^n \tag{2.30}$$

by the truncated filter

$$\bar{H}_a^i(Z_1,Z_2) = \sum_{m=0}^{M-1}\sum_{n=0}^{N-1} \bar{h}_{mn}^i Z_1^m Z_2^n , \tag{2.31}$$

where the conditions

$$\begin{aligned} \bar{h}_{mn}^i &= \tilde{h}_{mn}^i, \ (m,n) \in T \\ &= 0, \ (m,n) \notin T \end{aligned} \tag{2.32}$$

and

$$\tilde{h}_{mn}^i \longleftrightarrow |H_{k\ell}| \exp(j\varphi_{k\ell}^i) \tag{2.33}$$

are satisfied, is described in the following. The phase sequences of the high order filters are denoted by $\{\varphi_{k\ell}^i\}$ as in (2.33). As with the original algorithm every high order filter $\tilde{H}_a^i(Z_1,Z_2)$ has $\{|H_{k\ell}|\}$ as its amplitude sequence. An expression for the error between $\tilde{H}_a^i(Z_1,Z_2)$ and $\bar{H}_a^p(Z_1,Z_2)$ is

$$\tilde{I}^{ip} = \sum_{m=0}^{M-1}\sum_{n=0}^{N-1} (\tilde{h}_{mn}^i - \bar{h}_{mn}^p)^2 . \tag{2.34}$$

The error sequence of the modified phase correction algorithm is given by

$$\tilde{W} = \{\tilde{I}^{00}, \tilde{I}^{10}, \ldots, \tilde{I}^{ii}, \tilde{I}^{i+1,i}, \ldots\}. \tag{2.35}$$

In a manner analogous to the original algorithm, the first spatial sequence is generated from $\{|H_{k\ell}|\}$ and $\{\varphi^0_{k\ell}\}$, using the equation

$$\{\tilde{h}^0_{mn}\} = \text{IDFT}\ \{|H_{k\ell}|\exp(j\varphi^0_{k\ell})\}. \tag{2.36}$$

Further, the first two iterations of the modified algorithm are identical to the first two iterations of the algorithm of section IIA, meaning that

$$\tilde{h}^i_{mn} = h^i_{mn},$$

$$\bar{h}^i_{mn} = \hat{h}^i_{mn},$$

and

$$\tilde{I}^{ii} = I^{ii}$$

for $i = 0,1$. For $i = 2$ the equations above also hold, but for $i \geq 2$ we form a second truncated sequence $\{y^i_{mn}\}$ in each iteration by using

$$y^i_{mn} = \bar{h}^i_{mn} + b^i(\bar{h}^i_{mn} - \bar{h}^{i-1}_{mn}) \tag{2.37}$$

where b^i is a real number chosen to accelerate the convergence of the algorithm. It may be assumed that in the first steps of the present algorithm, b^0 and b^1 are zero. The number b^i is chosen so that the sum of squared errors,

$$K_i = \sum_{m=0}^{M-1}\sum_{n=0}^{N-1}(\bar{h}^i_{mn} - (\bar{h}^{i-1}_{mn} + b^i(\bar{h}^{i-1}_{mn} - \bar{h}^{i-2}_{mn})))^2, \tag{2.38}$$

between $\{\bar{h}^i_{mn}\}$ and $\{\bar{h}^{i-1}_{mn} + b^i(\bar{h}^{i-1}_{mn} - \bar{h}^{i-2}_{mn})\}$ is minimized. This is

achieved by differentiating (2.38) with respect to b^i and setting the result equal to zero. This gives

$$b^i = \frac{\sum_{m=0}^{M-1} \sum_{n=0}^{N-1} (\bar{h}^i_{mn} - \bar{h}^{i-1}_{mn})(\bar{h}^{i-1}_{mn} - \bar{h}^{i-2}_{mn})}{\sum_{m=0}^{M-1} \sum_{n=0}^{N-1} (\bar{h}^{i-1}_{mn} - \bar{h}^{i-2}_{mn})^2} . \tag{2.39}$$

Given the sequence $\{y^i_{mn}\}$, the operations

$$\{\bar{H}^i_{k\ell}\} = \text{DFT}\ \{y^i_{mn}\}, \tag{2.40}$$

$$i = i+1, \tag{2.41}$$

$$\tilde{H}^i_{k\ell} = |H_{k\ell}|\ (\bar{H}^{i-1}_{k\ell} / |\bar{H}^{i-1}_{k\ell}|), \tag{2.42}$$

and

$$\{\tilde{h}^i_{mn}\} = \text{IDFT}\ \{\tilde{H}^i_{k\ell}\} \tag{2.43}$$

are carried out for the implementation of the algorithm. This leaves the algorithm at the truncation step. Because of the way the sequences $\{y^i_{mn}\}$ are generated one cannot guarantee that

$$\tilde{I}^{ii} < \tilde{I}^{i-1,i-1}. \tag{2.44}$$

Therefore, if (2.44) doesn't hold, let

$$\bar{h}^i_{mn} = \bar{h}^{i-1}_{mn}, \tag{2.45}$$

$$b^i = 0, \tag{2.46}$$

and continue the iteration. In other words, if an iteration of the modified algorithm fails to produce a smaller error number than the previous iteration, we repeat the iteration with $b^i = 0$, which is equivalent to performing an iteration in the original algorithm. The final error sequence $\tilde{W}$ has the property that

$$\tilde{I}^{ii} \leq \tilde{I}^{i-1,i-1} \tag{2.47}$$

for all i greater than 0. If the iteration fails in the above fashion the value of the error function for two successive iterations is the same, meaning

$$\tilde{I}^{ii} = \tilde{I}^{i-1,i-1}. \tag{2.48}$$

However, this does not imply that the modified algorithm has converged. Whenever (2.45) is implemented, the equation

$$\bar{h}_{mn}^{i-1} = \bar{h}_{mn}^{i-2}$$

holds in the following iteration, giving a zero denominator in (2.39). This is easily remedied by replacing $\bar{h}_{mn}^{i-2}$ by $\bar{h}_{mn}^{i-3}$ in (2.39), in an iteration following the implementation of (2.45).

The block diagram for the modified phase correction algorithm is shown in Figure 2. As with the original algorithm, the numbers I_E and i_{max} provide exits. The steps of the algorithm are given below in detail. As seen in (2.39), b^i can't be calculated if $i < 2$. Therefore, (2.46) is used for $i = 0$ and 1.

Step 0: Given $\{|H_{k\ell}|\}$, $\{\varphi^0_{k\ell}\}$, T, I_E, and i_{max}, set i equal to zero and compute $\{\tilde{H}^0_{k\ell}\}$ using

$$\tilde{H}^0_{k\ell} = |H_{k\ell}|\exp(j\varphi^0_{k\ell}). \tag{2.49}$$

Step 1: Calculate $\{\tilde{h}^i_{mn}\}$ using (2.43).

Step 2: If (2.44) holds, continue to Step 3; otherwise skip to Step 6.

Step 3: Perform the truncation in (2.32).

Step 4: Exit if $\tilde{I}^{i-1,i-1} - \tilde{I}^{ii} < I_E$ or $i \geq i_{max}$.

Step 5: If $i < 2$ set $b^i = 0$; otherwise calculate b^i from (2.39); go to Step 7.

Step 6: Perform (2.45) and (2.46).

Step 7: Compute $\{y^i_{mn}\}$ using (2.37).

Step 8: Find $\{\bar{H}^i_{k\ell}\}$ from (2.40).

Step 9: Increase i by 1.

Step 10: Calculate $\{\tilde{H}^i_{k\ell}\}$ using (2.42).

Step 11: Go to Step 1.

It may be added that the extra steps of the modified algorithm do not add significantly to the computation time of an iteration. Although faster converging error sequences have been observed when using the modified algorithm, an analytical proof of the fast convergence is not available at this time. However, this approach is useful in many optimization problems where the dimensionality is too high for the Fletcher-Powell algorithm [14] to be practical.

C. An Alternate Derivation

It should be noted that the algorithm of Section IIA can be derived by applying a gradient [14] method of optimization to the error function

$$K(\{\hat{h}^{i-1}_{mn}\}) = \sum_{k=0}^{M-1} \sum_{\ell=0}^{N-1} (|H_{k\ell}| - |\hat{H}^{i-1}_{k\ell}|)^2 . \tag{2.50}$$

Using (2.6),

$$\frac{\partial \hat{H}^{i-1}_{k\ell}}{\partial \hat{h}^{i-1}_{pq}} = U^{pk} V^{q\ell}$$

and

$$\frac{\partial \hat{H}^{i-1*}_{k\ell}}{\partial \hat{h}^{i-1}_{pq}} = U^{-pk} V^{-q\ell} ,$$

lead to

$$\frac{\partial K(\{\hat{h}^{i-1}_{mn}\})}{\partial \hat{h}^{i-1}_{pq}} = -\Bigg(\sum_{k=0}^{M-1} \sum_{\ell=0}^{N-1} \Bigg(|H_{k\ell}| \frac{\hat{H}^{i-1}_{k\ell}}{|\hat{H}^{i-1}_{k\ell}|} U^{-pk} V^{-q\ell} - \hat{H}^{i-1}_{k\ell} U^{-pk} V^{-q\ell} \Bigg) + \Bigg(|H_{k\ell}| \frac{\hat{H}^{i-1*}_{k\ell}}{|\hat{H}^{i-1}_{k\ell}|} U^{pk} V^{q\ell} - \hat{H}^{i-1*}_{k\ell} U^{pk} V^{q\ell} \Bigg) \Bigg) . \tag{2.51}$$

Equations (2.15), (2.16), (2.24), and (2.51) yield

$$\frac{\partial K(\{\hat{h}^{i-1}_{mn}\})}{\partial \hat{h}^{i-1}_{pq}} = -2MN(h^{i}_{pq} - \hat{h}^{i-1}_{pq}) . \tag{2.52}$$

If the classical gradient method were being used to decrease $K(\{\hat{h}^{i-1}_{mn}\})$, the next step would be to implement

$$\hat{h}^{i}_{pq} = \hat{h}^{i-1}_{pq} + \rho \frac{\partial K(\{\hat{h}^{i-1}_{mn}\})}{\partial \hat{h}^{i-1}_{pq}} \quad , (p,q) \in T,$$

$$= 0, \ (p,q) \notin T, \tag{2.53}$$

where ρ is a negative number such that

$$\frac{\partial K(\{\hat{h}^{i}_{mn}\})}{\partial \rho} = 0 \ . \tag{2.54}$$

In the algorithm of Section IIA, (2.53) is implemented such that

$$\rho = -1/(2MN) \ . \tag{2.55}$$

It can be shown that (2.53) and (2.55) do not give the result of (2.54). Therefore, the phase correction algorithm is related to, but not the same as, the classical gradient technique.

Steiglitz, in [12], minimized an error function like that of (2.50) for one-dimensional recursive filters, using the Fletcher-Powell algorithm [14]. Unlike Steiglitz we did not use cascaded second order sections, but did use the FFT. We did not use the Fletcher-Powell algorithm because of storage considerations. In terms of real floating-point words, the storages of the original algorithm, the modified algorithm, and the Fletcher-Powell algorithm are

$$S_1 = (M_1+1)(N_1+1) + 2MN \tag{2.56}$$

$$S_2 = 3(M_1+1)(N_1+1) + 2MN \tag{2.57}$$

and

$$S_3 = ((M_1+1)(N_1+1))^2/2 + 5\tfrac{1}{2}(M_1+1)(N_1+1) + 2MN \tag{2.58}$$

respectively, where $(M_1 + 1)(N_1 + 1)$ is assumed to be even in (2.58). For $M_1 = N_1 = 7$ and $M = N = 32$,

$$S_1 = 2112,$$

$$S_2 = 2240,$$

and

$$S_3 = 4448.$$

Here, the Fletcher-Powell algorithm requires almost double the storage of the modified algorithm. If M, N, M_1, and N_1 are increased linearly, the amount of storage required for the Fletcher-Powell algorithm increases much faster than the amount of storage required by the modified algorithm. For both algorithms FFT calculations take up most of the computation time. Therefore, for each iteration, the computation time is approximately proportional to $MN\log_2 MN$.

D. Phase Sequences and Phase Error

In this section a technique for choosing the initial phase sequence $\{\theta^0_{k\ell}\}$ is formulated and a method of comparing the phase

sequence $\{\theta^i_{k\ell}\}$ to a set of desired phase sequences is developed. The following notation and observations are needed in this section.

The frequency response of the filter $H\hat{a}^i(Z_1, Z_2)$ is expressed in amplitude-phase form as

$$H\hat{a}^i(\exp(-j\omega_1), \exp(-j\omega_2))$$

$$= |H\hat{a}^i(\exp(-j\omega_1), \exp(-j\omega_2))| \exp(j\Omega^i(\omega_1, \omega_2)), \tag{2.59}$$

where $|H\hat{a}^i(\exp(-j\omega_1), \exp(-j\omega_2))|$ is the amplitude response and $\Omega^i(\omega_1, \omega_2)$ is the phase response. Salient properties of the frequency response are: (i) The symmetry conditions for the amplitude and phase responses are

$$|H\hat{a}^i(\exp(-j\omega_1), \exp(-j\omega_2))| = |H\hat{a}^i(\exp(j\omega_1), \exp(j\omega_2))| \tag{2.60}$$

and

$$\Omega^i(\omega_1, \omega_2) = \mu^i(\omega_1, \omega_2)2\pi - \Omega^i(-\omega_1, -\omega_2) \tag{2.61}$$

where $\mu^i(\omega_1, \omega_2)$ takes on integer values. Conditions (2.60) and (2.61) are necessary and sufficient for $\{h^i_{mn}\}$ to be a real sequence.
(ii) Linear phase responses for digital filters may be expressed as

$$\Omega^i(\omega_1, \omega_2) = -\alpha\omega_1/2 - \beta\omega_2/2 + \xi\pi/2 + \gamma^i(\omega_1, \omega_2)\pi \tag{2.62}$$

where α, β, and ξ are non-negative integer constants, with ξ equal to 0 or 1, and $\gamma^i(\omega_1, \omega_2)$ is a function taking on values 0 or 1. If $\xi = 1$

in (2.62), the filter is said to have negative symmetry and if $\xi = 0$, the filter has positive symmetry.

(iii) The results of this section are derived for filters with positive symmetry but they are easily derived for negatively symmetric filters as well.

If $H_a^i(Z_1, Z_2)$ has linear phase and positive symmetry, $\Omega^i(\omega_1, \omega_2)$ may be expressed as

$$\Omega^i(\omega_1, \omega_2) = -(K/2)\omega_1 - (L/2)\omega_2 + \gamma^i(\omega_1, \omega_2)\pi \tag{2.63}$$

where K and L are non-negative integers. If $h^i_{m,N-1}$, h^i_{n0}, h^i_{0k}, and $h^i_{M-1,\ell}$ are non-zero for some values of m, n, k, and ℓ, the only possible values of K and L in (2.63) are M-1 and N-1, respectively.

(iv) It is specifically assumed in this section that T is described by (1.11), meaning that (2.3) may be rewritten as

$$\hat{H}_a^i(Z_1, Z_2) = \sum_{m=0}^{M_1} \sum_{n=0}^{N_1} \hat{h}^i Z_1^m Z_2^n . \tag{2.64}$$

If $\hat{H}_a^i(Z_1, Z_2)$ is a linear phase filter with positive symmetry and if $\hat{h}^i_{n0}$, $\hat{h}^i_{mN_1}$, $\hat{h}^i_{0k}$, and $\hat{h}^i_{M_1\ell}$ are non-zero for some values of m, n, k, and ℓ, the phase response $\hat{\Omega}^i(\omega_1, \omega_2)$ of $\hat{H}_a^i(Z_1, Z_2)$ can be expressed as

$$\hat{\Omega}^i(\omega_1, \omega_2) = -(M_1/2)\omega_1 - (N_1/2)\omega_2 + \hat{\gamma}^i(\omega_1, \omega_2)\pi \tag{2.65}$$

where $\hat{\gamma}^i(\omega_1, \omega_2)$ is a function taking on values 0 or 1.

(v) The DFT that is used to get $\{H^i_{k\ell}\}$ from $\{h^i_{mn}\}$ and $\{\hat{H}^i_{k\ell}\}$ from $\{\hat{h}^i_{mn}\}$ is of order (M, N). This means that ω_1 and ω_2 are restricted by

$$\omega_1 = (2\pi/M)k, \quad 0 \le k \le M-1, \tag{2.66}$$

$$\omega_2 = (2\pi/N)\ell, \quad 0 \le \ell \le N-1, \tag{2.67}$$

and that

$$H^i_{k\ell} = H\hat{a}^i((2\pi/M)k, (2\pi/N)\ell),$$

$$\hat{H}^i_{k\ell} = \hat{Ha}^i((2\pi/M)k, (2\pi/N)\ell).$$

Thus from (2.63), (2.66), and (2.67) a positively symmetric linear phase filter, $H\hat{a}^i(Z_1, Z_2)$, has a phase sequence expressed as

$$\begin{aligned}\theta^i_{k\ell} &= \Omega^i((2\pi/M)k, (2\pi/N)\ell) \\ &= -(K/2)(2\pi/M)k - (L/2)(2\pi/N)\ell \\ &\quad + \gamma^i((2\pi/M)k, (2\pi/N)\ell)\pi.\end{aligned} \tag{2.68}$$

Let S^i be a subset of T_0 such that $(k, \ell) \epsilon S^i$ if $\gamma^i(2\pi/M)k, (2\pi/N)\ell) = 0$, $\notin S^i$ otherwise. Equation (2.68) can now be expressed as

$$\theta^i_{k\ell} = -(K/2)(2\pi/M)k - (L/2)(2\pi/N)\ell \tag{2.69}$$

for $(k, \ell) \epsilon S^i$ and

$$\theta^i_{k\ell} = -(K/2)(2\pi/M)k-(L/2)(2\pi/N)\ell + \pi \tag{2.70}$$

if $(k,\ell)\notin S^i$. It should be emphasized that a linear phase response implies a linear phase sequence; however a linear phase sequence such as (2.68) does not necessarily imply a linear phase response. For a filter $H^i_a(Z_1,Z_2)$ to have the linear phase response of (2.63), the necessary and sufficient coefficient constraint is

$$\begin{aligned} h^i_{mn} &= h^i_{K-m,L-n}, \quad m \le K \text{ and } n \le L, \\ &= 0 \qquad\quad , \quad m > K \text{ or } n > L. \end{aligned} \tag{2.71}$$

THEOREM 2: If the initial phase sequence $\{\theta^0_{k\ell}\}$ is described by (2.68), with $(K,L) = (M_1,N)$, every phase sequence $\{\theta^i_{k\ell}\}$ can also be described by (2.68) with $(K,L) = (M_1,N_1)$.

Proof: Let $(K,L) = (M_1,N_1)$ and let U and V be as defined in Chapter I. Note that

$$\exp(j\theta^i_{k\ell}) = U^{kM_1/2}\, V^{\ell N_1/2} \tag{2.72}$$

if $(k,\ell)\in S^i$ and

$$\exp(j\theta^i_{k\ell}) = -U^{kM_1/2}\, V^{\ell N_1/2} \tag{2.73}$$

if $(k,\ell)\notin S^i$. For $m \le M_1$ and $n \le N_1$, equations (2.4), (2.72), and (2.73) imply

$$\hat{h}^{i}_{mn} = (1/MN) \sum_{\substack{k=0 \\ (k,\ell)\in S^{i}}}^{M-1} \sum_{\ell=0}^{N-1} |H_{k\ell}| U^{-k(m-M_1/2)} V^{-\ell(n-N_1/2)}$$

$$-(1/MN) \sum_{\substack{k=0 \\ (k,\ell)\notin S^{i}}}^{M-1} \sum_{\ell=0}^{N-1} |H_{k\ell}| U^{-k(m-M_1/2)} V^{-\ell(n-N_1/2)} . \qquad (2.74)$$

The fact that $M_1 - m - M_1/2 = -(m-M_1/2)$ and $N_1 - n - N_1/2 = -(n-N_1/2)$ leads to

$$\hat{h}^{i}_{M_1-m,N_1-n} = (1/MN) \sum_{\substack{k=0 \\ (k,\ell)\in S^{i}}}^{M-1} \sum_{\ell=0}^{N-1} |H_{k\ell}| U^{k(m-M_1/2)} V^{\ell(n-N_1/2)}$$

$$-(1/MN) \sum_{\substack{k=0 \\ (k,\ell)\notin S^{i}}}^{M-1} \sum_{\ell=0}^{N-1} |H_{k\ell}| U^{k(m-M_1/2)} V^{\ell(n-N_1/2)}$$

$$= \hat{h}^{i*}_{mn} = \hat{h}^{i}_{mn} \qquad (2.75)$$

for $m \le M_1$ and $n \le N_1$. Using (2.68), (2.71), and (2.75)

$$\hat{\theta}^{i}_{k\ell} = -(M_1/2)(2\pi/M)k - (N_1/2)(2\pi/N)\ell + \hat{\gamma}^{i}((2\pi/M)k, (2\pi/N)\ell)\pi \quad . \qquad (2.76)$$

Equations (2.21) and (2.76) imply

$$\theta^{i+1}_{k\ell} = -(M_1/2)(2\pi/M)k - (N_1/2)(2\pi/N)\ell + \hat{\gamma}^{i}((2\pi/M)k, (2\pi/N)\ell)\pi \quad . \qquad (2.77)$$

Replacing $\hat{\gamma}^i((2\pi/M)k,(2\pi/N)\ell)$ by $\gamma^{i+1}((2\pi/M)k,(2\pi/N)\ell)$ in (2.77), $\{\theta^{i+1}_{k\ell}\}$ can be expressed by (2.68) if $\{\theta^{i}_{k\ell}\}$ can be expressed by (2.68), when $(K,L) = (M_1,N_1)$. Since $\{\theta^{0}_{k\ell}\}$ is described by (2.68) with $(K,L) = (M_1,N_1)$, the theorem holds by induction.

Q.E.D.

Corollary: If $\{\theta^{0}_{k\ell}\}$ is described by (2.68) and $(K,L) = (M_1,N_1)$, the error sequence W converges in a finite number of iterations.

Proof: Assuming $(K,L) = (M_1,N_1)$ and (2.68) holds for $i = 0$, theorem 2 implies (2.68) holds for every i. The function $\gamma^i((2\pi/M)k, (2\pi/N)\ell)$ takes on one of two values for every one of the MN ordered pairs (k,ℓ) in T_0. Therefore there are only 2^{MN} possible candidates for the function $\gamma^i((2\pi/M)k,(2\pi/N)\ell)$ and fewer than 2^{MN} when (2.19) holds. Since W is strictly decreasing before convergence and since different error values I^{ii} correspond to different phase sequences $\{\theta^{i}_{k\ell}\}$, there are fewer than 2^{MN} iterations.

Q.E.D.

The corollary to theorem 2 implies that if $\{\theta^{0}_{k\ell}\}$ is properly chosen the phase correction algorithm may be used to design linear phase response filters. However, in designing such filters, numerical problems in the FFT implementation of the DFT cause the symmetry condition of (2.71) to be violated. In other words

$$\hat{h}^i_{mn} = \hat{h}^i_{M_1-m,N_1-n} + \epsilon^i_{mn},\ m \le M_1 \text{ and } n \le N_1,$$

where $\{\epsilon^i_{mn}\}$ is an error sequence with non-zero members. The result

is that the phase sequences $\{\theta^i_{k\ell}\}$ may not be described by (2.68) and W does not converge in a finite number of iterations. This can be remedied by implementing the arithmetic replacement statement

$$\hat{h}^i_{mn} = \hat{h}^i_{M_1-m,N_1-n} = .5(\hat{h}^i_{mn} + \hat{h}^i_{M_1-m,N_1-n}).$$

In general the limit $I^{\infty\infty}$ of the sequence W depends upon the initial phase sequence $\{\theta^0_{k\ell}\}$, as illustrated in the section on numerical results. In other words, the algorithm converges to a local minimum rather than to a global minimum. It may be possible to guarantee convergence to a global minimum in the 1-D case by making use of minimum phase versions of the filter coefficient polynomials. However, polynomials of two or more dimensions generally do not have minimum phase versions and such a procedure cannot be extended to two or more dimensions. At present, the only way to insure that this error $I^{\infty\infty}$ is small is to pick $\{\theta^0_{k\ell}\}$ such that I^{00} is small. If I^{00} is small, the fact that W is non-increasing precludes the possibility that $I^{\infty\infty}$ is large.

Let

$$\theta^0_{k\ell} = -(2\pi/M)(K/2)k-(2\pi/N)(L/2)\ell+\pi\gamma_{k\ell}, \tag{2.78}$$

$$\gamma_{k\ell} = \begin{cases} 0 \text{ for K and L even,} \\ u(k-M/2) \text{ for K odd and L even,} \\ u(\ell-N/2) \text{ for K even and L odd,} \\ u(k-M/2) + u(\ell-N/2) \text{ for K and L odd,} \end{cases} \tag{2.79}$$

$$u(x) = \begin{cases} 0 \text{ for } x < 0, \\ 1 \text{ for } x \geq 0, \end{cases}$$

where K and L are non-negative integers which are to be chosen such that I^{00} is minimized. Typically, I^{00} is minimized for some (K,L) close to (M_1,N_1). However, if $(K,L) = (M_1,N_1)$, there are a finite number of iterations, using the corollary to theorem 2, and the limit of W is not much smaller than I^{00}. For this reason one should not use $(K,L) = (M_1,N_1)$ in (2.78) unless a linear phase response filter is mandatory.

Theorem 3: If $\{\theta^0_{k\ell}\}$ is specified by (2.78), then

$$I^{00} = E - 16 \sum_{m=0}^{M_1} \sum_{n=0}^{N_1} q^2_{[2m-K]_{2M},[2n-L]_{2N}} \tag{2.80}$$

where

$$q_{mn} \longleftrightarrow |H_{k\ell}| \exp(j\pi\gamma_{k\ell}) , \tag{2.81}$$

where $|H_{k\ell}| = 0$ for $k \geq M$ or $\ell \geq N$, and where the DFT is for sequences of length (2M,2N).

Proof: From (2.9) and (2.17),

$$I^{00} = E - \sum_{m=0}^{M_1} \sum_{n=0}^{N_1} (h^0_{mn})^2 . \tag{2.82}$$

Equation (2.78) leads to $\exp(j\theta^0_{k\ell}) = U^{kK/2} V^{\ell L/2} \exp(j\pi\gamma_{k\ell})$

and therefore, using $\tilde{U} = \exp(-j2\pi/2M)$ and $\tilde{V} = \exp(-j2\pi/2N)$,

$$h^0_{mn} = (1/MN) \sum_{k=0}^{M-1} \sum_{\ell=0}^{N-1} |H_{k\ell}| U^{-k(m-K/2)} V^{-\ell(n-L/2)} \exp(j\pi\gamma_{k\ell})$$

$$= (4/(2M2N)) \sum_{k=0}^{2M-1} \sum_{\ell=0}^{2N-1} |H_{k\ell}| \tilde{U}^{-k(2m-K)} \tilde{V}^{-\ell(2n-L)} \exp(j\pi\gamma_{k\ell})$$

$$= 4\, q_{[2m-K]_{2M},[2n-L]_{2N}}. \qquad (2.83)$$

On substituting $4q_{[2m-K]_{2M},[2n-L]_{2N}}$ for h^0_{mn} in (2.82) one obtains the result.

Q.E.D.

After using the IDFT to find $\{q_{mn}\}$ one can easily find from (2.80) the values of K and L for which I^{00} is minimized.

With the exception of the special case of theorem 2 and its corollary the phase sequences $\{\theta^i_{k\ell}\}$ produced by the phase correction algorithm are in general nonlinear. Linear phase sequences are usually desirable and it is therefore profitable to compare the actual phase sequences $\{\theta^i_{k\ell}\}$ to linear phase sequences. Let the linear phase sequences, which we shall compare the actual phase sequences to, be described by

$$\varphi^d_{k\ell} = \delta\pi - (2\pi/M)(K/2)k - (2\pi/N)(L/2)\ell + \pi\gamma_{k\ell} \qquad (2.84)$$

and (2.79) where K, L, and δ are non-negative integer variables and δ is 0 or 1. A convenient measure for the error between $\{\theta^i_{k\ell}\}$ and the linear phase sequences $\{\varphi^d_{k\ell}\}$ is

$$J_1 = \min_{\delta,K,L} \left(\sum_{k=0}^{M-1} \sum_{\ell=0}^{N-1} |H_{k\ell}|^2 \left|\exp(j\varphi^d_{k\ell}) - \exp(j\theta^i_{k\ell})\right|^2 \right). \qquad (2.85)$$

Two advantages in using J_i as a measure of phase error are:
(i) phase differences of 2π are equivalent to zero phase differences and
(ii) phase errors in pass regions are weighted more heavily than phase errors in transition and reject regions.

Suppose that for some positive Δ smaller than π,

$$|\varphi^d_{k\ell} - \theta^i_{k\ell}| = \Delta \ , \ (k,\ell) \in T_0. \tag{2.86}$$

Equation (2.86) implies that the error between $\{\theta^i_{k\ell}\}$ and a linear phase sequence equals Δ at each of the MN DFT points in the frequency domain, and that

$$\theta^i_{k\ell} = \varphi^d_{k\ell} \pm \Delta \ , \ (k,\ell) \in T_0. \tag{2.87}$$

If (2.86) holds and (2.87) is substituted into (2.85), the fact that

$|\exp(j\varphi^d_{k\ell}) - \exp(j(\varphi^d_{k\ell} + \Delta))|^2 = 2(1-\cos(\Delta))$ implies that

$$\begin{aligned} J_i &= \sum_{k=0}^{M-1} \sum_{\ell=0}^{N-1} |H_{k\ell}|^2 \, 2(1-\cos(\Delta)) \\ &= 2(1-\cos(\Delta)) \sum_{k=0}^{M-1} \sum_{\ell=0}^{N-1} |H_{k\ell}|^2 \\ &= 2MNE(1-\cos(\Delta)). \end{aligned} \tag{2.88}$$

For a given value of Δ, if

$$J_i \leq 2MNE(1-\cos(\Delta)) \tag{2.89}$$

then

$$|\varphi^{d}_{k\ell} - \theta^{i}_{k\ell}| \leq \Delta \tag{2.90}$$

will probably not be true for all (k,ℓ) in T_0, but it will tend to be true in the pass regions, since the error in the pass regions contributes heavily to the value of J_i.

Given that (2.90) is desired for some positive $\Delta \leq \pi$, J_i can be calculated every few iterations and the algorithm can be halted when (2.89) is not satisfied. If the initial phase sequence is a linear one such as given in (2.78), (2.89) will hold at least for $i = 0$.

It is assumed that the specific values of δ, K, and L in (2.84) are not of critical importance. If the values are needed, they are easily determined by using the following theorem.

Theorem 4: For given values of E and $\{H^{i}_{k\ell}\}$,

$$J_i = 2MN(E - \max_{m,n}(|R_{mn}|))$$

where

$$R_{mn} \longleftrightarrow |H_{k\ell}|H^{i}_{k\ell} \text{ for K and L even,}$$

$$R_{mn} \longleftrightarrow |H_{k\ell}|H^{i}_{k\ell}U^{k/2}\exp(j\pi\gamma_{k\ell}) \text{ for K odd and L even,}$$

$$R_{mn} \longleftrightarrow |H_{k\ell}|H^{i}_{k\ell}V^{\ell/2}\exp(j\pi\gamma_{k\ell}) \text{ for K even and L odd,}$$

and

$$R_{mn} \longleftrightarrow |H_{k\ell}|H^{i}_{k\ell}U^{k/2}V^{\ell/2}\exp(j\pi\gamma_{k\ell}) \text{ for K and L odd.}$$

Proof: We prove the theorem for K and L even. The proofs for the other cases are similar. From (2.84), (2.85), and (2.9)

$$J_1 = 2 \sum_{k=0}^{M-1} \sum_{\ell=0}^{N-1} |H_{k\ell}|^2 - 2\max_{\delta, K, L} \left(\sum_{k=0}^{M-1} \sum_{\ell=0}^{N-1} |H_{k\ell}| H^i_{k\ell} \exp(-j\varphi^d_{k\ell}) \right)$$

$$= 2(MN E - \max_{\delta, K, L} ((-1)^\delta \sum_{k=0}^{M-1} \sum_{\ell=0}^{N-1} |H_{k\ell}| H^i_{k\ell} U^{-kK/2} V^{-\ell L/2} .$$

Replacing (K/2, L/2) by (m,n) leads to

$$J_1 = 2MN(E - \max_{m,n} (|(1/(MN)) \sum_{k=0}^{M-1} \sum_{\ell=0}^{N-1} |H_{k\ell}| H^i_{k\ell} U^{-km} V^{-\ell n}|) .$$

Q.E.D.

In theorem 4 we show how to measure phase error in a filter. In the following chapter we show how to measure the effects of this phase error on filtered pictures.

III. THE MEASUREMENT OF PHASE DISTORTION

A. Derivation of the Measure

In this section we develop a measure of phase distortion, and give a few of its properties. Let $\{p_{mn}\}$ be an output picture, with M rows and N columns, satisfying

$$p_{mn} \longleftrightarrow P_{k\ell} \tag{3.1}$$

and having a Fourier transform $P(\omega_1, \omega_2)$ as described in (1.17). $\{P_{k\ell}\}$ is a sampling of one period of $P(\omega_1, \omega_2)$ at MN points. $\{P_{k\ell}\}$ satisfies the radial symmetry condition

$$P_{k\ell} = P^*_{[M-k]_M, [N-\ell]_N} \quad . \tag{3.2}$$

The output picture $\{\hat{p}_{mn}\}$, which has the Fourier transform $\hat{P}(\omega_1, \omega_2)$ described in (1.19), satisfies

$$\hat{p}_{mn} \longleftrightarrow \hat{P}_{k\ell} \quad , \tag{3.3}$$

$$|\hat{P}_{k\ell}| = |P_{k\ell}| \quad , \tag{3.4}$$

$$\hat{P}_{k\ell} = P_{k\ell} \exp(jm_{k\ell}) \quad , \tag{3.5}$$

and

$$m_{k\ell} = m((2\pi/M)k, (2\pi/N)\ell) \quad , \tag{3.6}$$

where $m(\omega_1,\omega_2)$ is given in (1.20).

A measure of phase distortion in $\{\hat{p}_{mn}\}$, due to the effects of $m(\omega_1,\omega_2)$, is

$$\hat{D}(p,\hat{p}) = \frac{\sum_{m=0}^{M-1}\sum_{n=0}^{N-1}(p_{mn}-\hat{p}_{mn})^2}{2\sum_{m=0}^{M-1}\sum_{n=0}^{N-1}p_{mn}^2} \tag{3.7}$$

which is the normalized squared Euclidean distance between $\{p_{mn}\}$ and $\{\hat{p}_{mn}\}$. The measure $\hat{D}(p,\hat{p})$ can be expressed in the frequency domain as

$$\hat{D}(p,\hat{p}) = \frac{\sum_{k=0}^{M-1}\sum_{\ell=0}^{N-1}|P_{k\ell}-\hat{P}_{k\ell}|^2}{2\sum_{k=0}^{M-1}\sum_{\ell=0}^{N-1}|P_{k\ell}|^2} \quad . \tag{3.8}$$

Filtering shifts the output with respect to the input. The fact that a shifted picture is recognizably the same as one which has not been shifted means that we must remove the effects of shifts due to filtering from $\hat{D}(p,\hat{p})$. The phase response of a filter which linearly shifts the output with respect to the input is

$$\Omega(\omega_1,\omega_2) = -(K/2)\omega_1 - (L/2)\omega_2 \tag{3.9}$$

where K and L are non-negative integers. The phase sequence $\{\tilde{\varphi}_{k\ell}\}$, derived from (3.9), is

$$\tilde{\varphi}_{k\ell} = -(K/2)(2\pi/M)k - (L/2)(2\pi/N)\ell + \pi\gamma_{k\ell} \tag{3.10}$$

where $\gamma_{k\ell}$ is given in (2.79).

From (3.10) and the definitions of U and V,

$$\exp(j\tilde{\varphi}_{k\ell}) = U^{kK/2} V^{\ell L/2} \exp(j\pi\gamma_{k\ell}) \quad . \tag{3.11}$$

In addition to its shifting effect, filtering can cause the output picture to be close to or equal to the negative of the input picture. We can remove this effect from $\hat{D}(p,\hat{p})$ by using a variable δ which equals ± 1. Based upon these observations our measure of phase distortion is

$$D(p,\hat{p}) = \frac{\min_{\delta,K,L} \sum_{k=0}^{M-1} \sum_{\ell=0}^{N-1} |P_{k\ell}\exp(j\tilde{\varphi}_{k\ell}) - \delta\hat{P}_{k\ell}|^2}{2 \sum_{k=0}^{M-1} \sum_{\ell=0}^{N-1} |P_{k\ell}|^2} \quad . \tag{3.12}$$

This measure $D(p,\hat{p})$ has the property

$$0 \le D(p,\hat{p}) \le 1 \quad .$$

Two advantages to using $D(p,\hat{p})$ as a measure of phase distortion are:

(i) phase differences of 2π are equivalent to zero phase differences and

(ii) the amplitude sequence weights the phase differences.

B. Evaluation and Application of $D(p,\hat{p})$

In this section we show how to evaluate $D(p,\hat{p})$ and how to use it in judging filter phase responses.

Theorem 5: Given $\{P_{k\ell}\}$, $\{\hat{P}_{k\ell}\}$, M, and N,

$$D(p,\hat{p}) = 1 - (\max_{m,n} |b_{mn}|)/\hat{E}$$

where

$$\hat{E} = (1/MN) \sum_{k=0}^{M-1} \sum_{\ell=0}^{N-1} |P_{k\ell}|^2 , \tag{3.13}$$

$$b_{mn} \longleftrightarrow P^*_{k\ell}\hat{P}_{k\ell} \text{ for K and L even,}$$

$$b_{mn} \longleftrightarrow P^*_{k\ell}\hat{P}_{k\ell}U^{k/2}V^{\ell/2}\exp(j\pi\gamma_{k\ell}) \text{ for K and L odd,}$$

$$b_{mn} \longleftrightarrow P^*_{k\ell}\hat{P}_{k\ell}U^{k/2}\exp(j\pi\gamma_{k\ell}) \text{ for K odd and L even, and}$$

$$b_{mn} \longleftrightarrow P^*_{k\ell}\hat{P}_{k\ell}V^{\ell/2}\exp(j\pi\gamma_{k\ell}) \text{ for K even and L odd.} \tag{3.14}$$

Proof: The proof is for K and L even. The proofs for K and/or L odd follow similarly. Equation (3.12) yields

$$D(p,\hat{p}) = \frac{\min_{\delta,K,L} \sum_{k=0}^{M-1} \sum_{\ell=0}^{N-1} |P_{k\ell}|^2 + |\hat{P}_{k\ell}|^2 - 2\delta P^*_{k\ell}\hat{P}_{k\ell}\exp(-j\tilde{\varphi}_{k\ell})}{2 \sum_{k=0}^{M-1} \sum_{\ell=0}^{N-1} |P_{k\ell}|^2}$$

which can be simplified, using (3.11) and (3.13), to give

$$D(p,\hat{p}) = \frac{\hat{E} - \max_{\delta,K,L} \delta\left((1/MN) \sum_{k=0}^{M-1} \sum_{\ell=0}^{N-1} P^*_{k\ell}\hat{P}_{k\ell}U^{-kK/2}V^{-\ell L/2}\right)}{\hat{E}} .$$

Replacing K/2 by m and L/2 by n and using (3.14) for K and L even we have

$$D(p,\hat{p}) = 1 - \left(\max_{m,n,\delta} (\delta b_{mn})\right)/\hat{E} .$$

The variable δ can be eliminated by an absolute value, giving

$$D(p,\hat{p}) = 1 - (\max_{m,n}|b_{mn}|)/\hat{E} \quad .$$

Q.E.D.

Given an example picture $\{p_{mn}\}$ and several sequences, $\{m_{k\ell}\}$, of phase distortion numbers, equations (3.3) - (3.5) can be used to generate degraded pictures $\{\hat{p}_{mn}\}$ and the corresponding values of D can be calculated using theorem 5. With the values of D and the degraded pictures, we can determine how large D can get before the picture $\{\hat{p}_{mn}\}$ is unrecognizable. We denote the largest allowable value of $D(p,\hat{p})$ as D_m.

We have shown how to calculate $D(p,\hat{p})$ when the output picture frequency characteristics $\{P_{k\ell}\}$ and $\{\hat{P}_{k\ell}\}$ are given. In the following we show how to calculate $D(p,\hat{p})$ when the frequency characteristics of the input picture and filter are given. The DFT versions of (1.17) and (1.19) are

$$P_{k\ell} = F_{k\ell}|H_{k\ell}|\exp(j\theta^{d}_{k\ell}) \tag{3.15}$$

and

$$\hat{P}_{k\ell} = F_{k\ell}|H_{k\ell}|\exp(j\theta_{k\ell}) \tag{3.16}$$

where

$$H_{k\ell} = H((2\pi/M)k,(2\pi/N)\ell) \quad ,$$

$$\theta^d_{k\ell} = \theta^d((2\pi/M)k, (2\pi/N)\ell) \quad ,$$

and

$$\theta_{k\ell} = \theta((2\pi/M)k, (2\pi/N)\ell) \quad .$$

Notice that the factor $P^*_{k\ell}\hat{P}_{k\ell}$ occurs in each of the expressions of (3.14). Using (3.13), (3.15) and (3.16),

$$\hat{E} = (1/MN) \sum_{k=0}^{M-1} \sum_{\ell=0}^{N-1} |F_{k\ell}|^2 |H_{k\ell}|^2 \tag{3.17}$$

and

$$P^*_{k\ell}\hat{P}_{k\ell} = |F_{k\ell}|^2 |H_{k\ell}|^2 \exp(j(\theta_{k\ell} - \theta^d_{k\ell})) \quad . \tag{3.18}$$

It is interesting to note that the amplitude of $\{F_{k\ell}\}$, but not its phase, is used in (3.17) and (3.18). $D(p,\hat{p})$ may be calculated using (3.17), (3.18), and theorem 5, given only $\{|F_{k\ell}|\}$, $\{|H_{k\ell}|\}$, $\{\theta^d_{k\ell}\}$, and $\{\theta_{k\ell}\}$. To find out whether or not a filter has an acceptable phase response, we may calculate $D(p,\hat{p})$ for the filter and several input pictures or test patterns. If $D(p,\hat{p})$ tends to be greater than D_m the filter is not useful. This testing procedure uses much computation time and storage if M and N are large.

Equations (3.5), (3.15) and (3.16) correspond to circular convolution and theorem 5 requires the evaluation of a circular correlation. Also, the frequency responses $\exp(jm(\omega_1,\omega_2))$, $H(\omega_1,\omega_2)$ and $\tilde{H}(\omega_1,\omega_2)$ generally correspond to an infinite number of filter coefficients, implying that M and N should be infinite. However, our main

purpose is to find and use $D(p,\hat{p})$ rather than to filter pictures, so circular convolution and circular correlation are acceptable.

C. Estimation of $D(p,\hat{p})$

When sampling $H(\omega_1,\omega_2)$ to produce $\{H_{k\ell}\}$, M and N may equal 128, for example, and be large enough for the representation to be accurate. However, when $|F(\omega_1,\omega_2)|$ and $P(\omega_1,\omega_2)$ are sampled to produce $\{|F_{k\ell}|\}$ and $\{P_{k\ell}\}$, M and N are typically equal to the picture's dimensions, which may be much larger than 128 by 128. If the input spectrum $|F(\omega_1,\omega_2)|$ is modeled by a smooth function $|\tilde{F}(\omega_1,\omega_2)|$, which is accurately represented by a small number of samples, we can greatly reduce M and N and estimate $D(p,\hat{p})$, thereby saving storage and computation time.

The Fourier transform of a one-dimensional pulse is a sinc function which dies off as $1/\omega$ and has a value of 1 for $\omega = 0$. Similarly [15] the two-dimensional Fourier transform of a disk shaped pulse dies off approximately as $1/R$ where

$$R = (\omega_1^2 + \omega_2^2)^{1/2} \quad . \tag{3.19}$$

A simple model of the input picture amplitude response $|F(\omega_1,\omega_2)|$ is

$$|\tilde{F}(\omega_1,\omega_2)| = 1/(1 + aR) \tag{3.20}$$

which dies out approximately as $1/R$. The constant a may be varied until the approximation is accurate. The digital version of $|\tilde{F}(\omega_1,\omega_2)|$ is $\{|\tilde{F}_{k\ell}|\}$, which is defined by

$$|\tilde{F}_{k\ell}| = |\tilde{F}(\omega_1,\omega_2)| \quad .$$

$$\omega_1 = \begin{cases} (2\pi/M)k, & k \le M/2 \\ (2\pi/M)k-2\pi, & k > M/2 \end{cases},$$

$$\omega_2 = \begin{cases} (2\pi/N)\ell, & \ell \le N/2 \\ (2\pi/N)\ell-2\pi, & \ell > N/2 \end{cases}.$$

Replacing $\{|F_{k\ell}|\}$ by $\{|\tilde{F}_{k\ell}|\}$ in (3.17) and (3.18), we may use theorem 5 to calculate $\tilde{D}(p,\hat{p})$, an estimate of $D(p,\hat{p})$. In general $|\tilde{F}(\omega_1,\omega_2)|$ is a much smoother function than $|F(\omega_1,\omega_2)|$, allowing us to reduce M and N, save storage, and save computation time.

The estimation technique of this section greatly simplifies the testing procedure for filter phase responses of section IIIB. Assume that $|\tilde{F}(\omega_1,\omega_2)|$ is a model for all input picture amplitude spectrums $|F(\omega_1,\omega_2)|$ of interest to us. To test the phase response of a filter we can compute $\tilde{D}(p,\hat{p})$ one time and compare it to D_m. When a filter is designed by the method of Chapter II $\tilde{D}(p,\hat{p})$ may be calculated at each iteration. When $\tilde{D}(p,\hat{p})$ becomes larger than D_m, the design algorithm may be terminated.

IV. NUMERICAL RESULTS

A. Filter Design Examples

The numerical implementation of algorithms described in Chapter II, together with the design of filters and a comparison of their frequency responses is presented in this section. The computation was performed on the CDC-6600 at The University of Texas at Austin. The pictures are printed in 16 grey levels with darker levels representing more positive quantities. For every grey level picture the range between the maximum and minimum intensities, of the function being displayed, was linearly divided into the 16 levels. Except for the linear phase response filters, every filter was designed in 100 iterations, with $i_{max} = 99$ and $I_E = 0$.

Example 1 The desired amplitude response is a ring described by

$$A(\omega_1, \omega_2) = 1, \ 1 < (\omega_1^2 + \omega_2^2)^{1/2} \leq 2 \qquad (4.1)$$

$$= .02 \ \text{otherwise},$$

where $|\omega_1| \leq \pi$ and $|\omega_2| \leq \pi$. The values of M, N, M_1, N_1 are 32, 32, 7, and 7, respectively. The amplitude sequence $\{|H_{k\ell}|\}$ is shown in Figure 3. Using the initial phase sequence of (2.78) with K and L determined from theorem 3 to be 8, Filter 1.1 was designed by the algorithm of section IIA and Filter 1.2 was designed by the modified algorithm of section IIB. The amplitude and phase responses of Filter 1.2 are shown in Figures 4 and 5, respectively. The responses of Filter 1.1 are almost identical to those of Filter 1.2, and are not given. The coefficients of

Filters 1.1 and 1.2 are presented in Tables 1 and 2. The initial and final error numbers for Filters 1.1 and 1.2 are normalized using the number E and given by

$$(I^{00}/E) = (\tilde{I}^{00}/E) \approx .13185 \quad , \tag{4.2}$$

$$(I^{99,99}/E) \approx .10368 \quad , \tag{4.3}$$

and

$$(\tilde{I}^{99,99}/E) \approx .102859 \quad . \tag{4.4}$$

One gets an idea of the rate of convergence of I^{ii} and $\tilde{I}^{ii}$ as $i \to 99$ from the plot of log $((I^{ii}/E) - .1028)$ and log $((\tilde{I}^{ii}/E) - .1028)$ versus i, given in Figure 6. As the figure shows, the modified algorithm's error sequence $\tilde{W}$ is nearer convergence after 40 iterations than the original algorithm's error sequence W after 100 iterations. The coefficients of Filters 1.1 and 1.2, in Tables 1 and 2, are significantly different. Filter 1.3, also with the desired amplitude sequence of Figure 3, had the linear initial phase sequence of (2.78) with $(K,L) = (M_1,N_1) = (7,7)$. The filter was designed using the original algorithm and its amplitude and phase responses are given in Figures 7 and 8. The coefficients are given in Table 3. The error sequence W, for this filter, converged at the fourth iteration, which is in agreement with the corollary to theorem 2. The normalized error numbers for Filter 1.3 are

$$(I^{00}/E) \approx .1374 \tag{4.5}$$

and

$$(I^{3,3}/E) \approx .1302 \quad . \tag{4.6}$$

As predicted by theorem 2, the phase response of Figure 8 is linear. The error numbers of (4.5) and (4.6) show that $\hat{Ha}^3(Z_1, Z_2)$ is not significantly better than $\hat{Ha}^0(Z_1, Z_2)$. The final filter is usually a small improvement over the original filter when (2.78) holds and $(K, L) = (M_1, N_1)$.

Comparing Figures 4 and 7, one can see that Filter 1.2, with the nonlinear phase, has a significantly smaller magnitude of ripple in the reject regions. Whereas Filter 1.3 has four distinct ripples in its passband, the passband ripple of Filter 1.2 is not detectable in the figure. The passband rejectband boundaries are distinctly diamond shaped for Filter 1.3 but are more nearly circular for Filter 1.2. Comparing Figures 5 and 8, one can see that the phase response of Filter 1.2 is not wild in the passband, but fairly linear.

Filter 1.4 was obtained by windowing Filter 1.3. Each coefficient $\hat{h}^3_{mn}$ of Filter 1.3 was replaced by $\hat{h}^3_{mn} w_{mn}$ in Filter 1.4, where

$$w_{mn} = 1 - \alpha r_{mn}/R \quad ,$$

$$r_{mn} = [(m - M_1/2)^2 + (n - N_1/2)^2]^{1/2} \quad ,$$

$$R = [(M_1/2)^2 + (N_1/2)^2]^{1/2} \quad ,$$

and

$$\alpha = .6 \quad .$$

The window in this example is a generalization of a window found in [8]. The amplitude response of Filter 1.4 is shown in Figure 9. Comparing Figures 7 and 9, it is apparent that although windowing reduces amplitude response ripples it also decreases the steepness of the response in transition regions.

Example 2 For this example the desired amplitude response is

$$A(\omega_1,\omega_2) = 1, \ |\omega_1| + |\omega_2| \leq 2.1$$
$$= 0, \quad \text{otherwise} \tag{4.7}$$

where $|\omega_1| \leq \pi$ and $|\omega_2| \leq \pi$. This corresponds to a low-pass filter with a diamond shaped passband. Both filters of this example were designed by the modified algorithm with M, N, M_1 and N_1 equal to 64, 64, 7, and 7, respectively. The desired amplitude sequence for the filters is shown in Figure 10.

The initial phase sequence of Filter 2.1 was (2.78) with (K,L) = (8,6), using theorem 3. The amplitude and phase responses of Filter 2.1 are given in Figures 11 and 12 and the coefficients are presented in Table 4. The normalized error numbers for Filter 2.1 are

$$(\tilde{I}^{00}/E) \approx .08691 \tag{4.8}$$

and

$$(\tilde{I}^{99,99}/E) \approx .08198 \ . \tag{4.9}$$

For Filter 2.2 the initial phase sequence was that of (2.78) with (K,L) = (63,63). The amplitude and phase responses are displayed

in Figures 13 and 14 and the coefficients are presented in Table 5. Plots of $\{|\tilde{h}^{0}_{mn}|\}$ and $\{|\tilde{h}^{99}_{mn}|\}$ for this filter are given in Figures 15 and 16. The normalized error numbers for the filter are

$$(\tilde{I}^{00}/E) \approx .99852 \tag{4.10}$$

and

$$(\tilde{I}^{99,99}/E) \approx .10098 \ . \tag{4.11}$$

It is apparent from (4.10) and (4.11) that the final filter is greatly improved over the initial filter. Figures 15 and 16 show that most of the coefficient energy is concentrated in those points corresponding to the set T. However, (4.9), (4.11), Figure 11 and Figure 13 indicate that Filter 2.2 has a much larger error number and a worse amplitude response than Filter 2.1. Also, $\tilde{I}^{00}$ for Filter 2.1 is smaller than $\tilde{I}^{99,99}$ for Filter 2.2. This illustrates the value of choosing a good initial phase sequence.

The values of M=N=32 in example 1 and M=N=64 in example 2 represent fairly coarse frequency sampling. For the examples we have chosen, however, larger values of M and N make no substantial difference.

B. Phase Distortion Examples

In this section we distort the phase of a test pattern by the method of (3.3 - 3.5) and by filtering and we then measure D for the degraded images. The actual values of D are compared to estimates obtained through the modeling procedure of section IIIC.

Example 3 Using (3.3 - 3.5) we distorted the phase of the spoke test pattern, $\{p_{mn}\}$, of Figure 17 with three zero mean Gaussian noise sequences $\{m_{k\ell}\}$. The sequences differ only in their standard deviations (i.e., the sequences are multiples of each other). The resulting pictures $\{\hat{p}_{mn}\}$ for standard deviations of .13, 375 and 1.0 are shown in Figures 18 through 20 respectively. The corresponding values of $D(p,\hat{p})$ are: .0096, .0787 and .32.

It is apparent from the figures that as a picture's phase is distorted its energy is redistributed in the spatial domain. This is a type of smearing.

Example 4 As a second example we distorted the phase of $\{p_{mn}\}$ in Figure 17 using the deterministic function

$$m(\omega_1,\omega_2) = .9(\omega_1^2 + \omega_2^2)^{1/2}(\omega_1 + \omega_2) \quad . \tag{4.12}$$

The resulting picture $\{\hat{p}_{mn}\}$, shown in Figure 21, corresponds to

$$D(p,\hat{p}) = .0779 \quad . \tag{4.13}$$

It is apparent that although the deterministic distortion of Figure 21 differs from the random distortion of Figure 19, the figures are equally recognizable as spoke patterns and the values of D for the two figures are about the same.

Example 5 As a third example we filtered the test pattern of Figure 17 using Filters 1.2 and 1.3. The desired amplitude response for both filters is given in (4.1) and the desired phase response is that of (3.9) with $K = L = 7$.

For Filter 1.2 the actual value of D, with $M = N = 128$, is

$$D(p,\hat{p}) = .078 \tag{4.14}$$

and the output picture is shown in Figure 22. For Filter 1.3 the actual value of D, with $M = N = 128$ is

$$D(p,\hat{p}) = .00974 \tag{4.15}$$

and the output picture is shown in Figure 23.

From (4.14), Filter 1.2 produces about the same amount of phase distortion as that seen in Figure 19. From Figure 19 one can correctly infer that the phase distortion seen in Figure 22 is moderate. If opposing spokes in Figure 22 are compared it is noticed that, unlike the spoke pattern of Figure 17, this filtered spoke pattern lacks radial symmetry. From (4.15), Filter 1.3 produces almost the amount of phase distortion seen in Figure 18. Although Figure 18 reflects a noticeable amount of phase distortion it is not easily detectable because Filter 1.3 has linear phase and Figure 23 has radial symmetry.

For both filters, the values of $D(p,\hat{p})$ were estimated using the method of section IIIC with $M = N = 32$ and $a = 32$. In Figures 24 and 25 respectively, $\{|F_{k\ell}|\}$ and our model $\{|\tilde{F}_{k\ell}|\}$ are shown for $M = N = 128$. a is picked to be 32 for the model so that the dark regions in Figures 24 and 25 are approximately the same in area. For Filter 1.2 our estimate of D is

$$\tilde{D}(p,\hat{p}) = .07334 \tag{4.16}$$

while for Filter 1.3 our estimate of D is

$$D(p,\hat{p}) = .00926 \ . \tag{4.17}$$

Comparing (4.14) to (4.16) and (4.15) to (4.17) we see that the estimation procedure of section IIIC works well for our examples.

V. CONCLUSION

By allowing the desired phase sequence of a filter to vary, while the desired amplitude sequence is held constant, one can significantly improve the filter's amplitude sequence. The phase correction algorithm always converges and its convergence can be considerably speeded. Because of the simplicity of this design method, it is relatively fast, with good filters being designed in less than 30 sec. for $M = N = 32$. Through the use of theorem 3 good initial phase sequences may be picked. An easily applied DFT correlation theorem makes it simple to measure the phase error between the actual filter and a linear phase version of it.

As our examples show, it is possible to measure the phase distortion, due to filtering, in digital pictures. Using the measure, the acceptability of filter phase responses can be determined. Using a simple model of input picture amplitude responses, the measure D may be estimated.

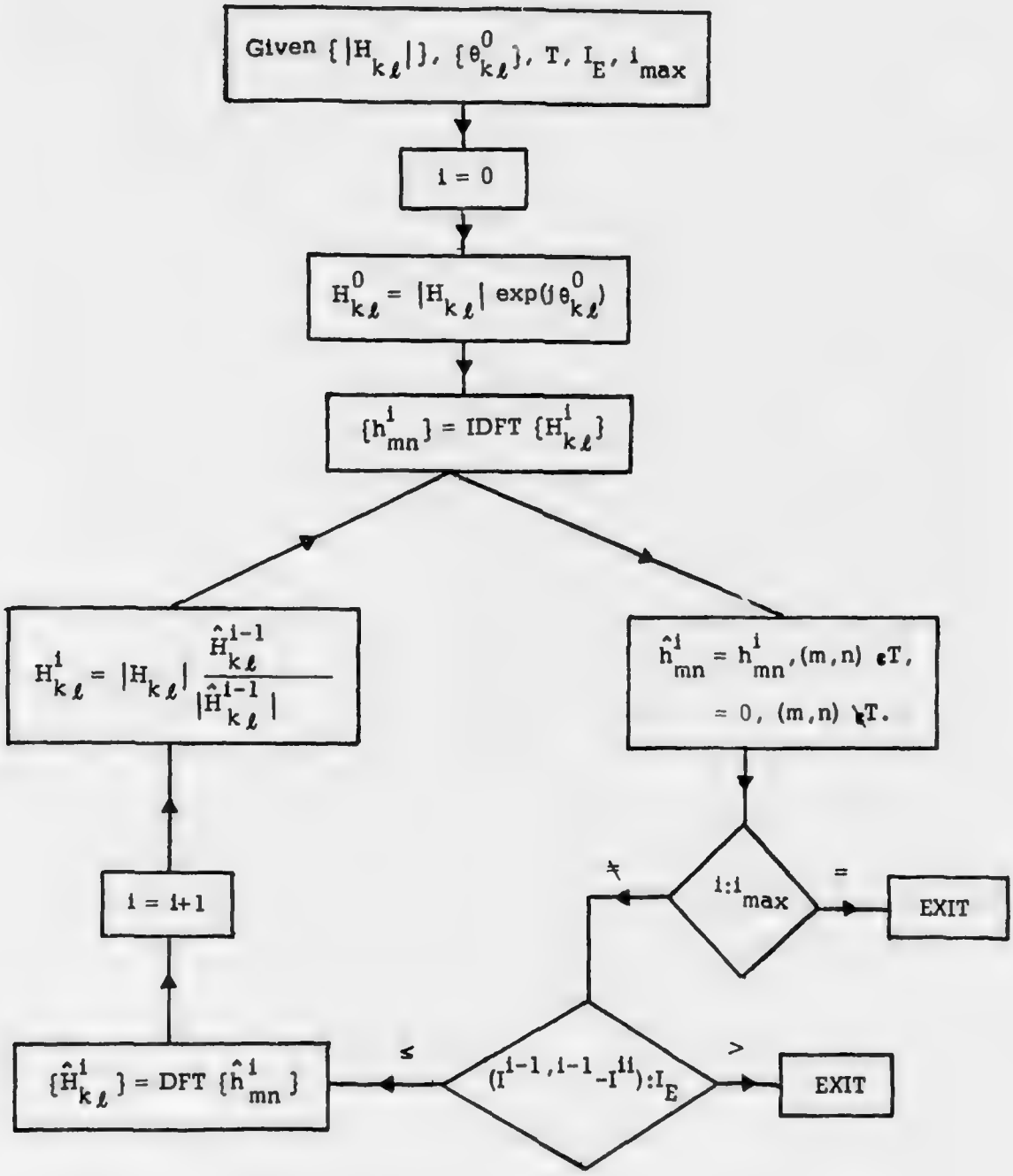

Figure 1. Block Diagram for the Original Algorithm

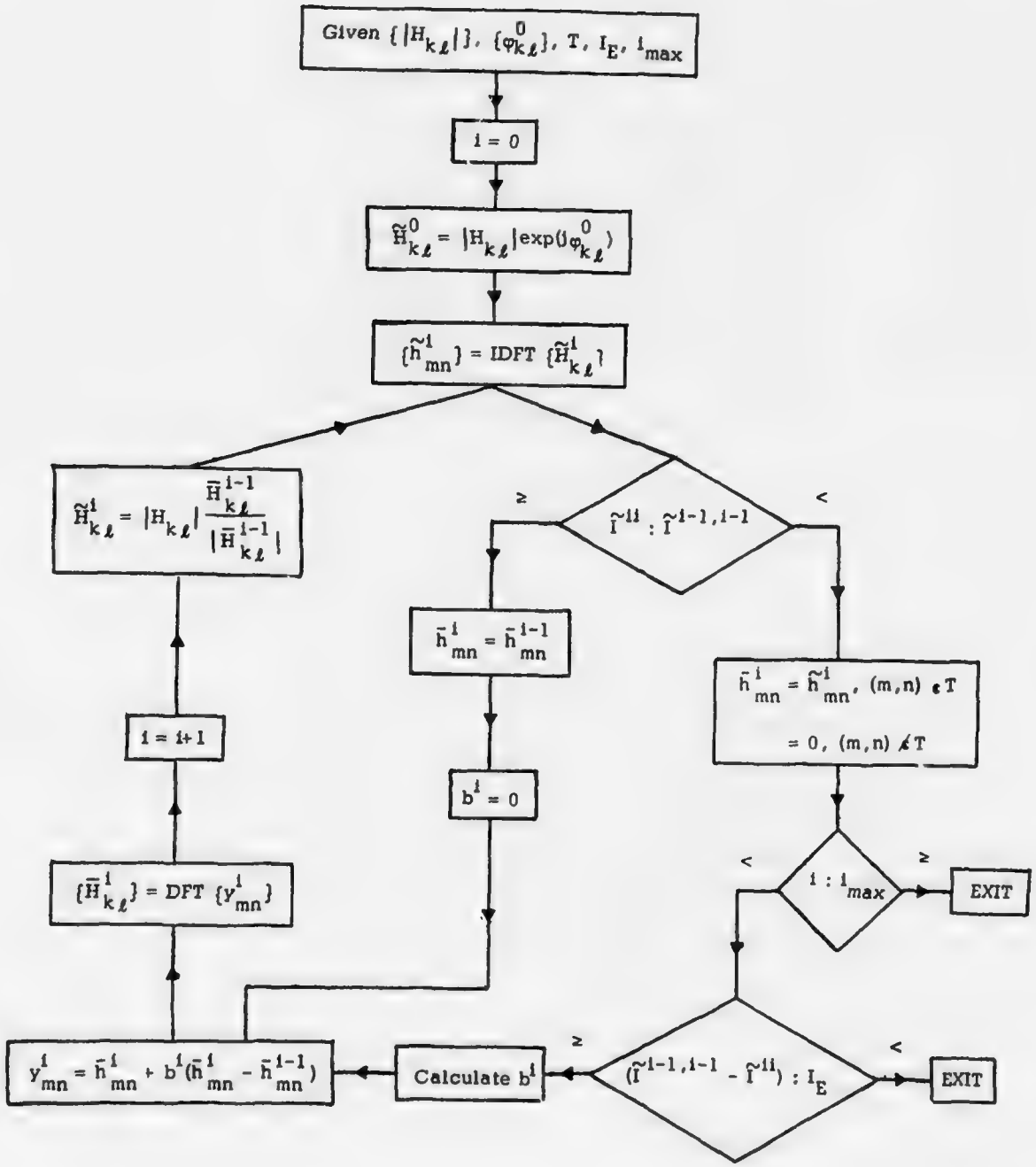

Figure 2. Block Diagram for the Modified Algorithm

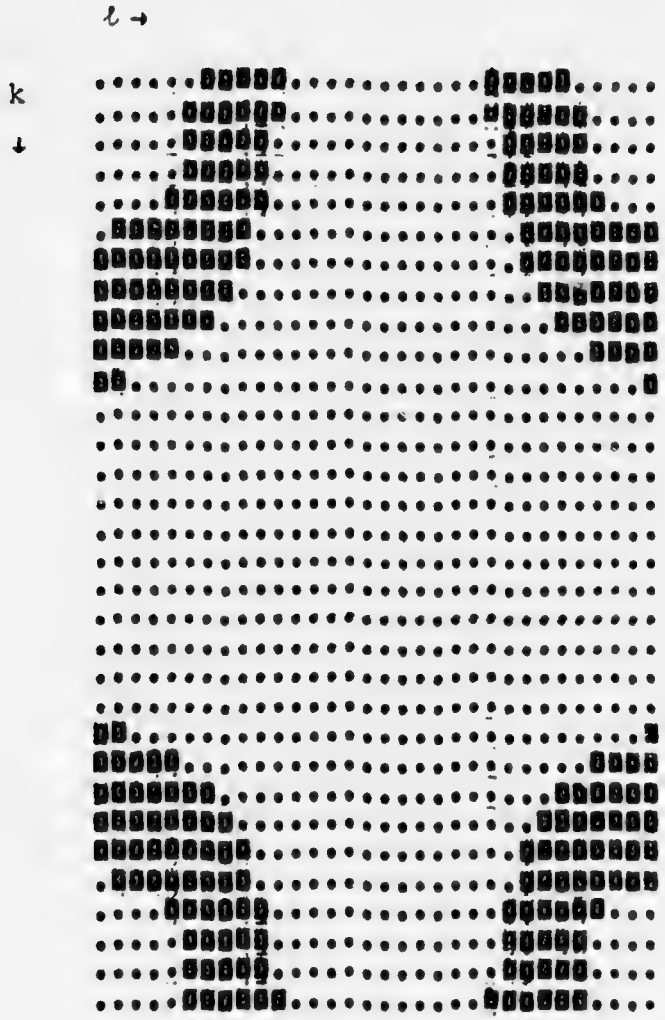

Figure 3. $\{|H_{k\ell}|\}$ For Filters 1.1, 1.2, and 1.3.

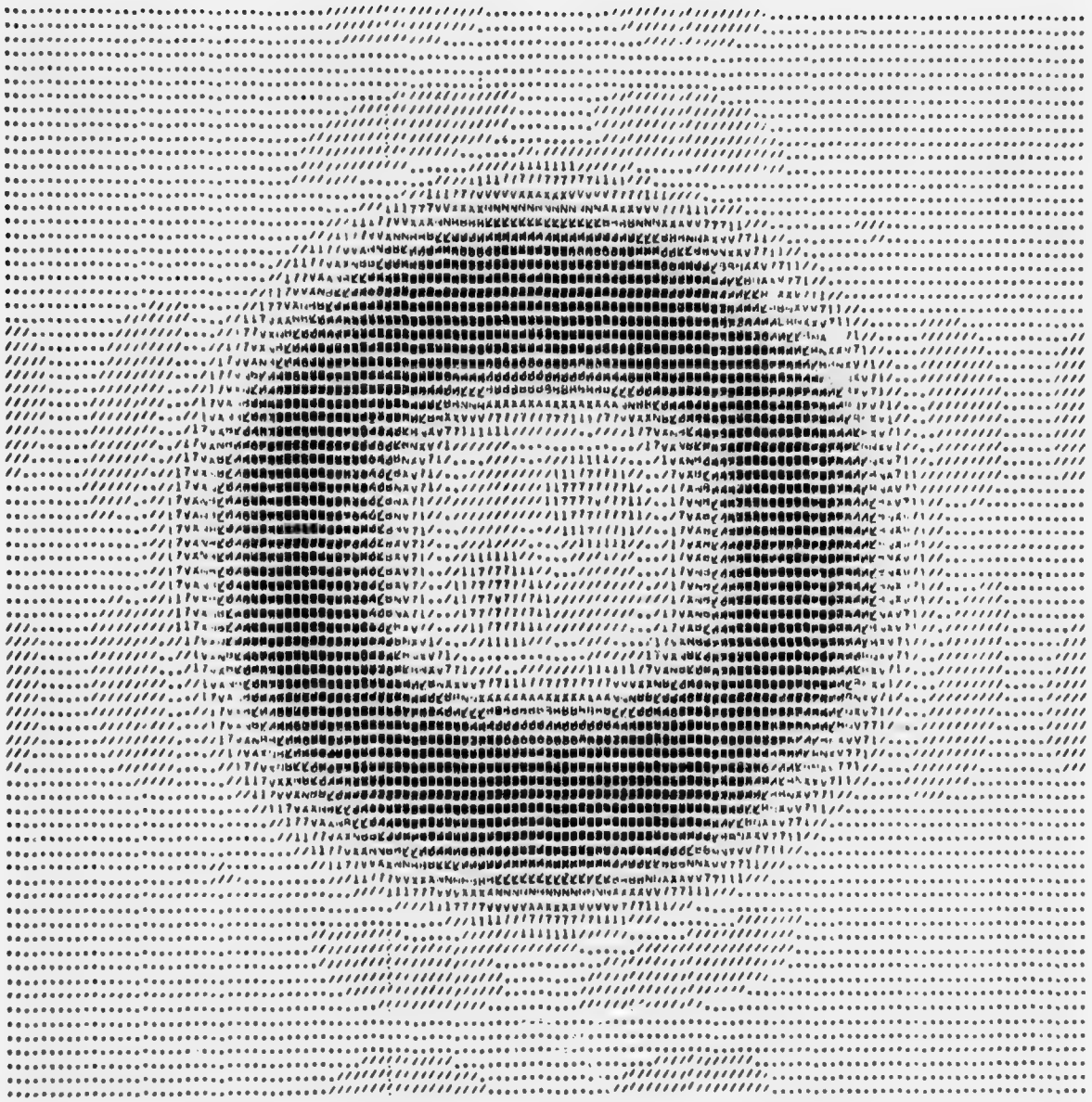

Figure 4. Amplitude Response of Filter 1.2.

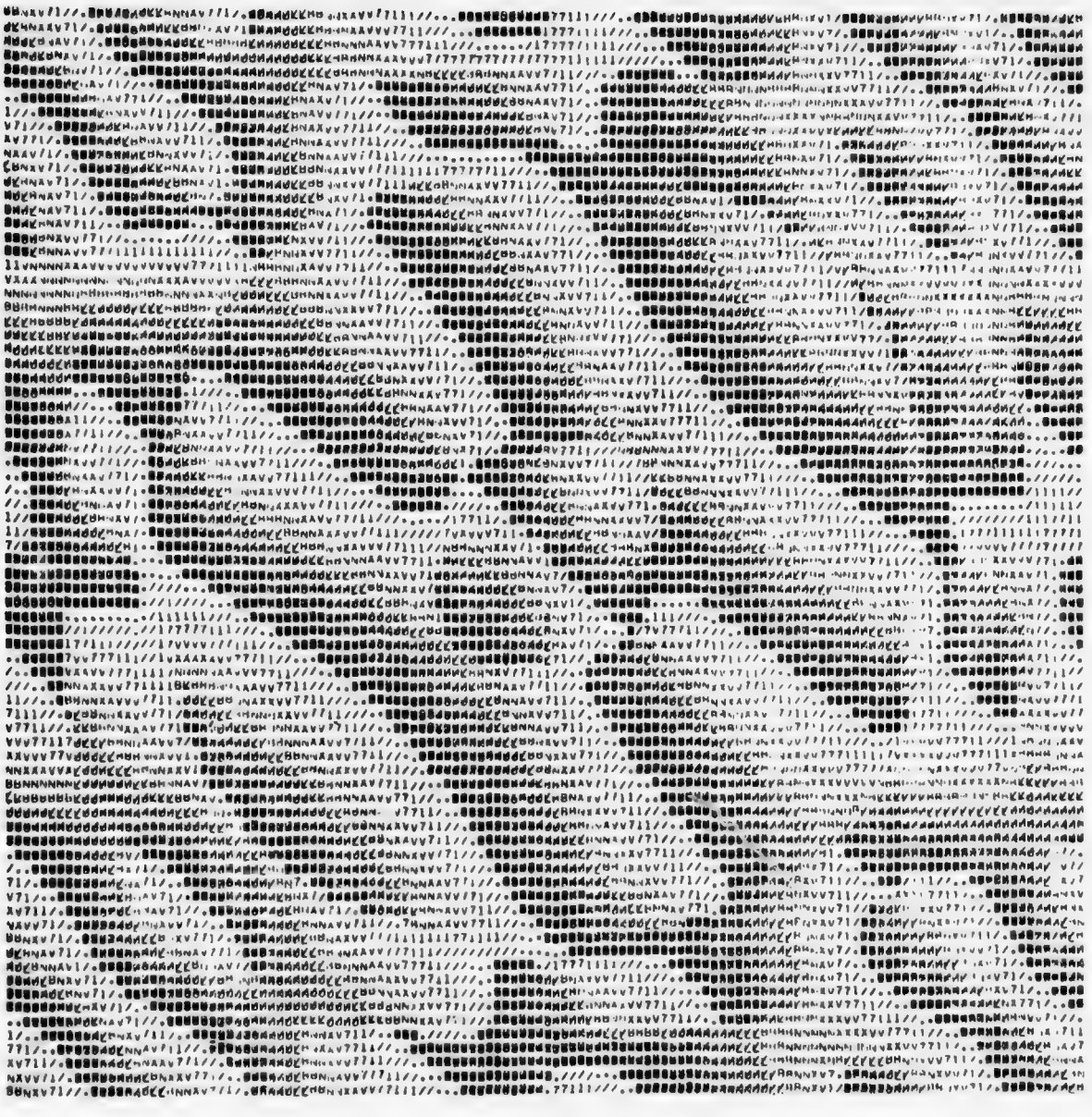

Figure 5. Phase Response of Filter 1.2.

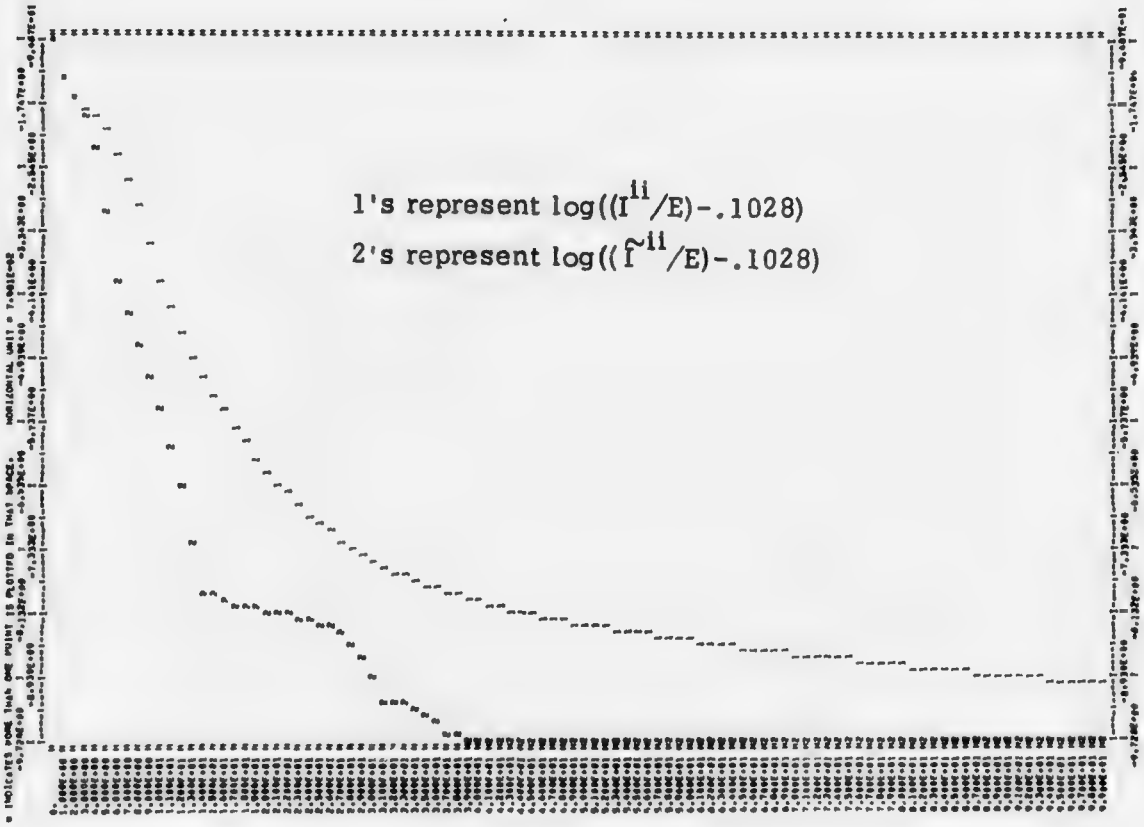

Figure 6. Plot of $\log((I^{ii}/E)-.1028)$ and $\log((\tilde{I}^{ii}/E)-.1028)$ Versus i For Filters 1.1 and 1.2.

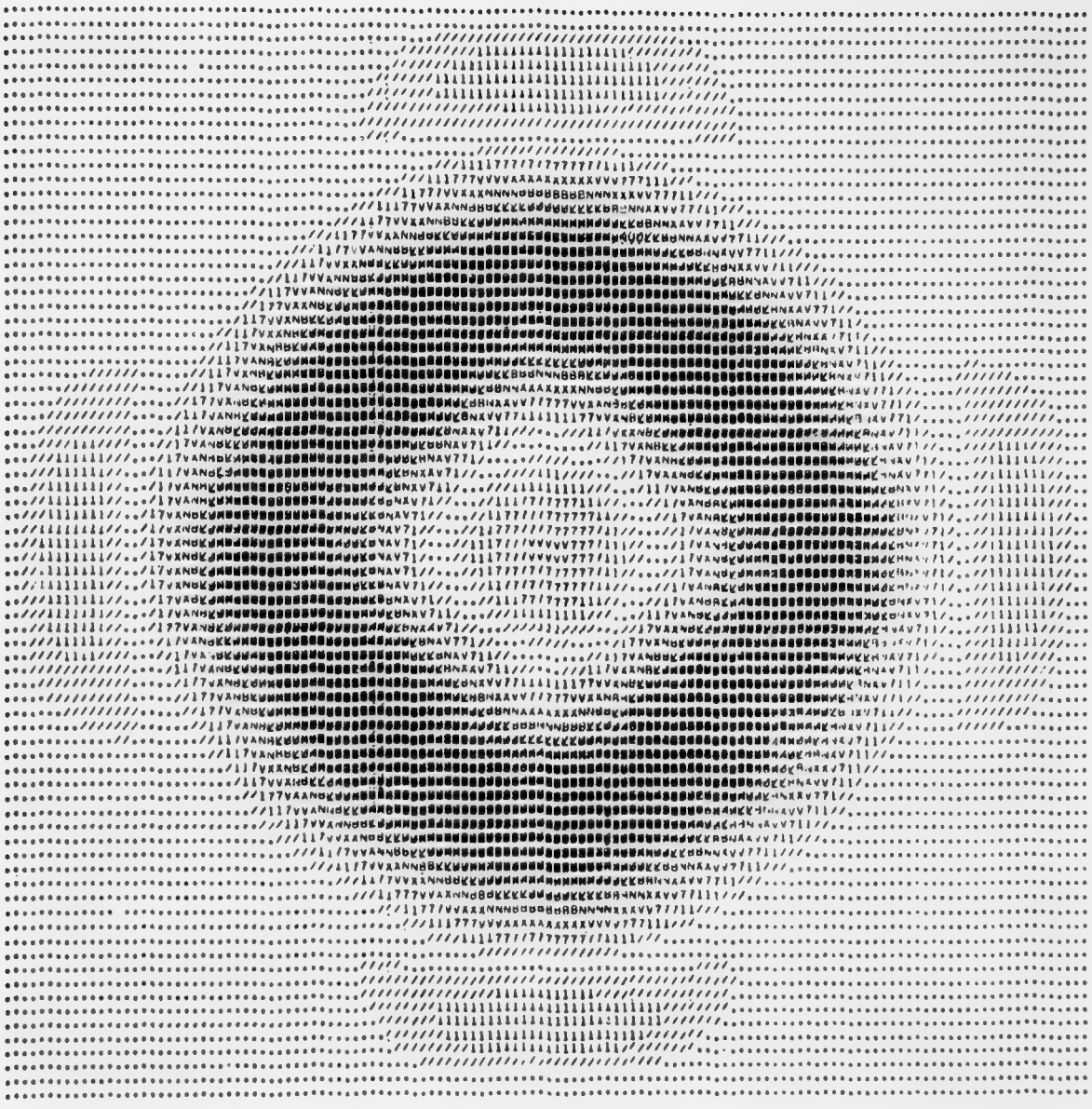

Figure 7. Amplitude Response of Filter 1.3.

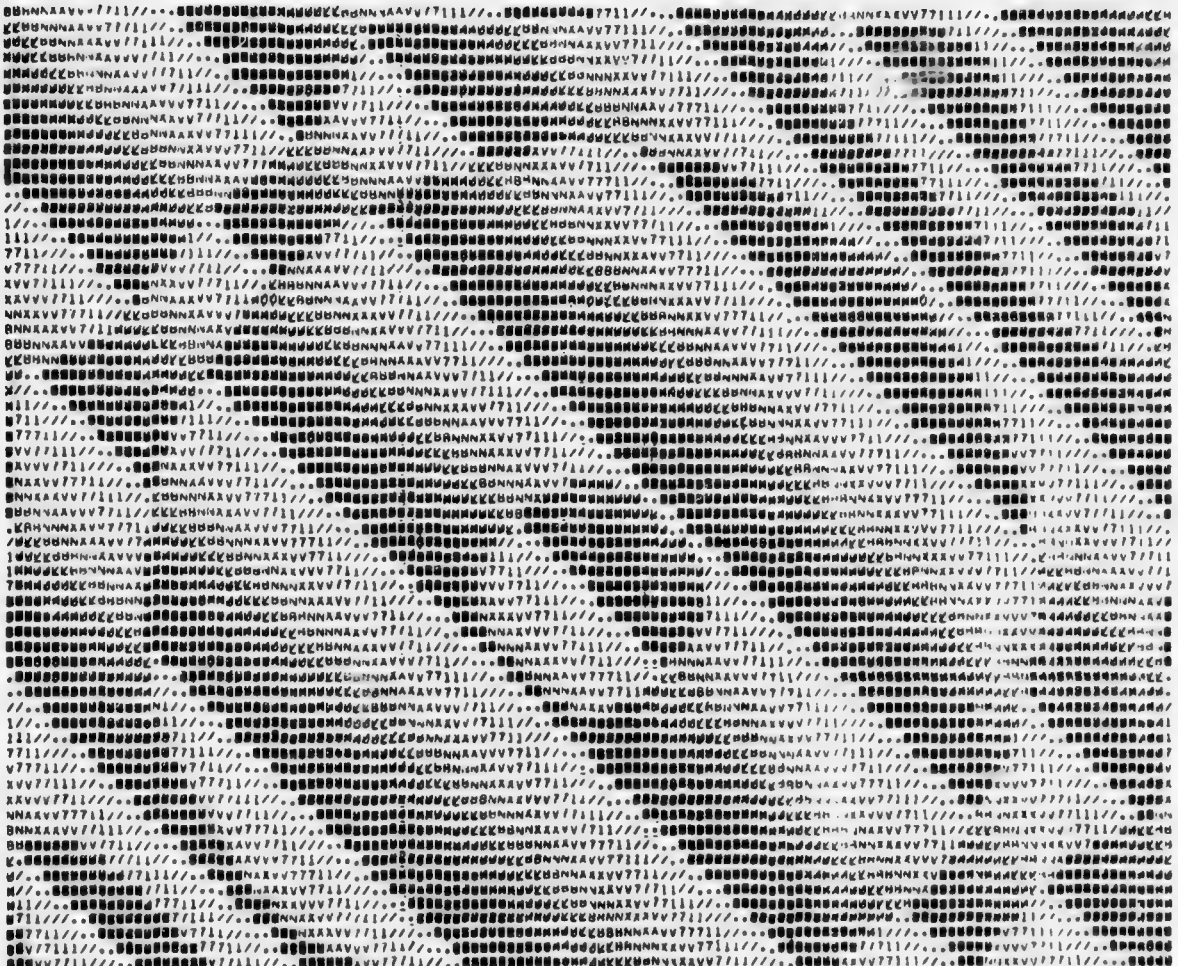

Figure 8. Phase Response of Filter 1.3.

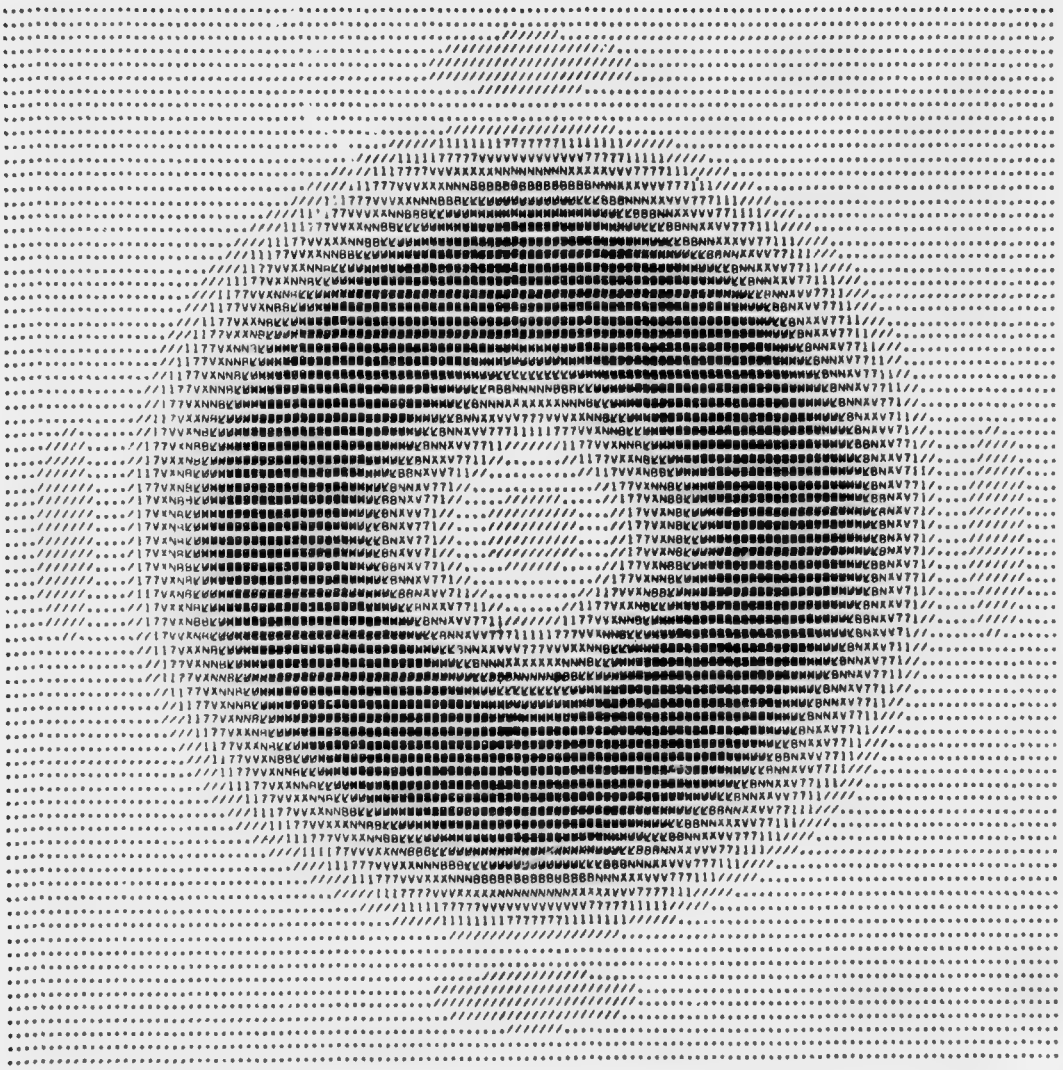

Fig. 9. Amplitude Response of Filter 1.4.

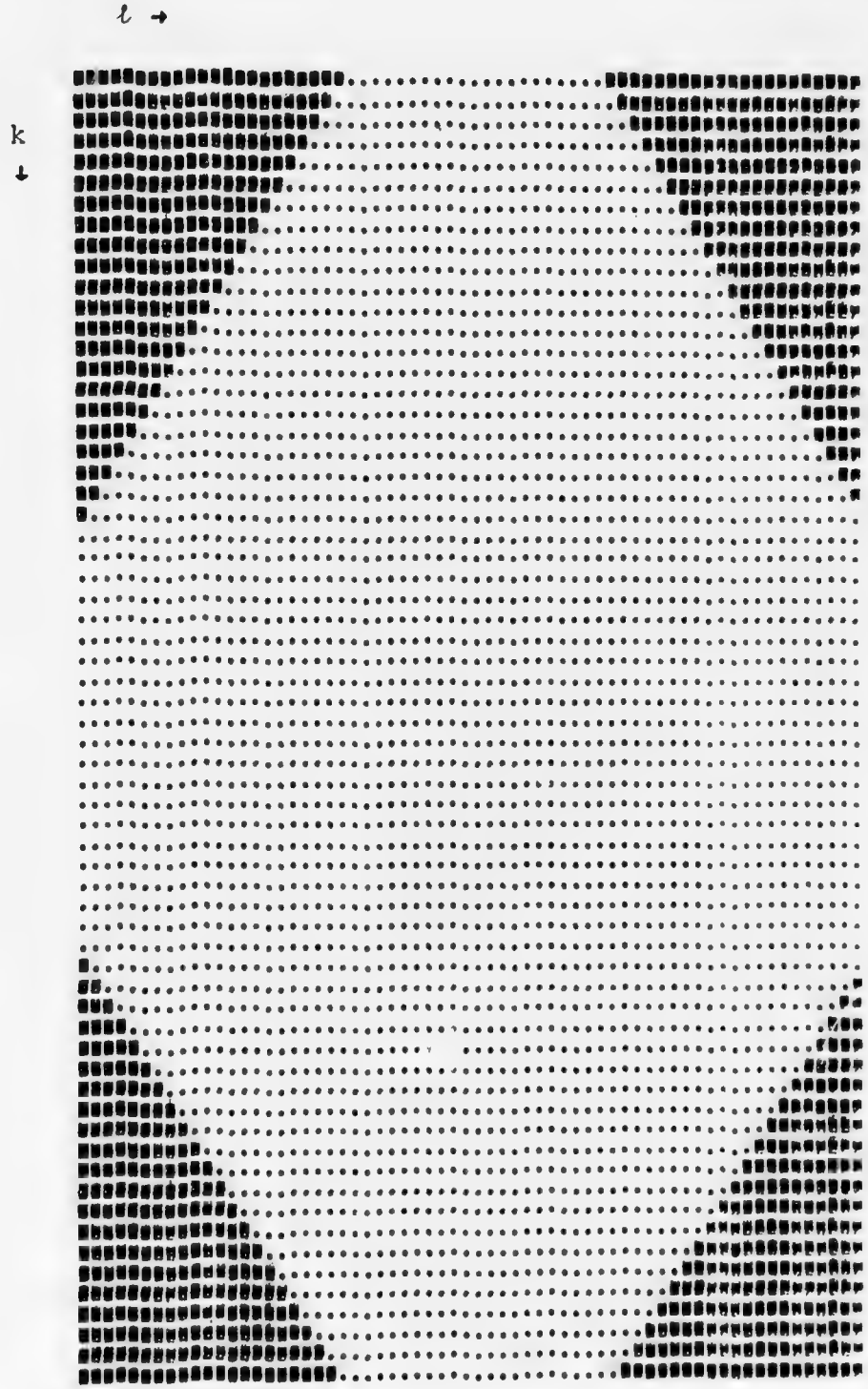

Figure 10. $\{|H_{k\ell}|\}$ For Filters 2.1 and 2.2.

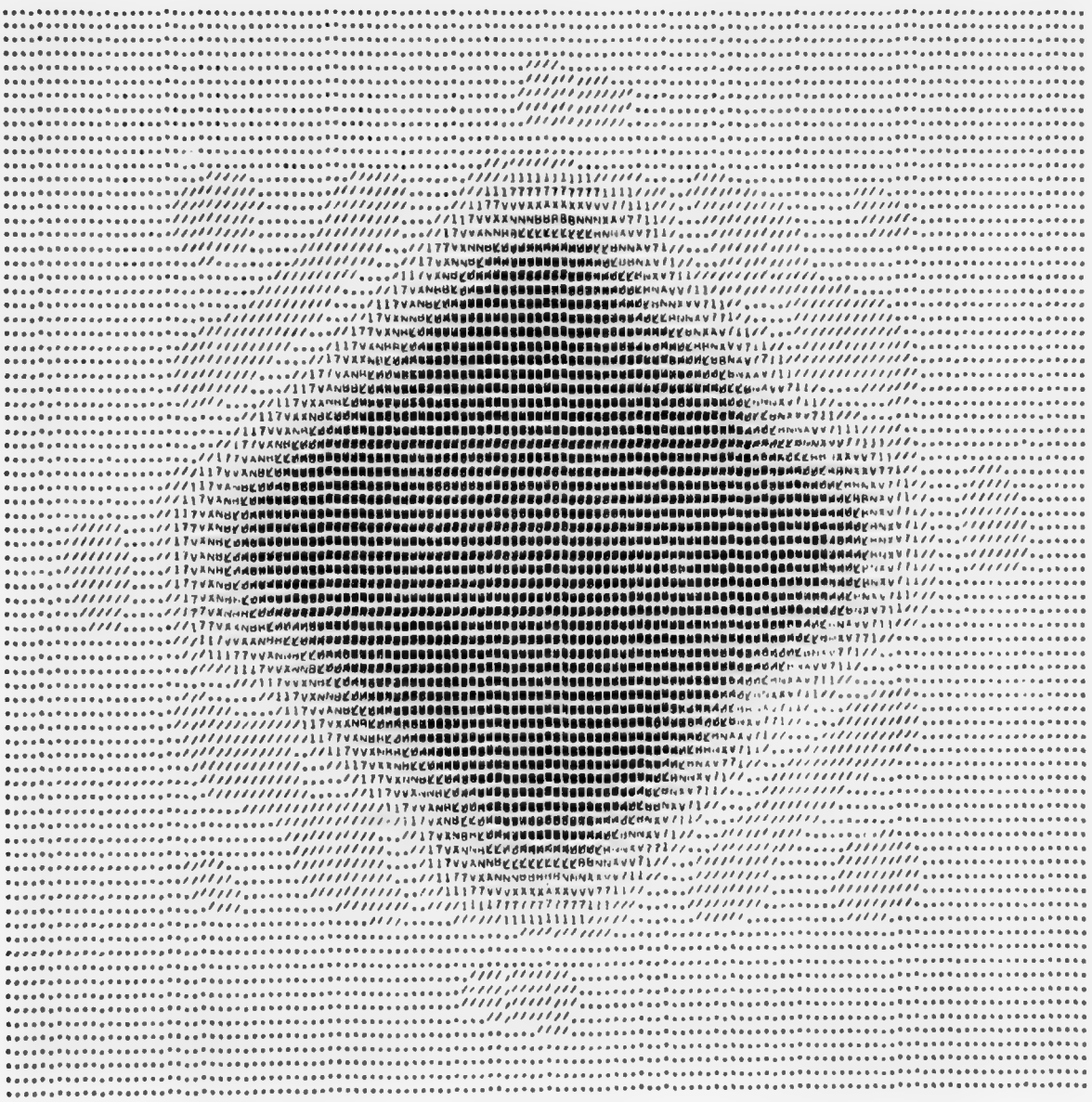

Figure 11. Amplitude Response of Filter 2.1.

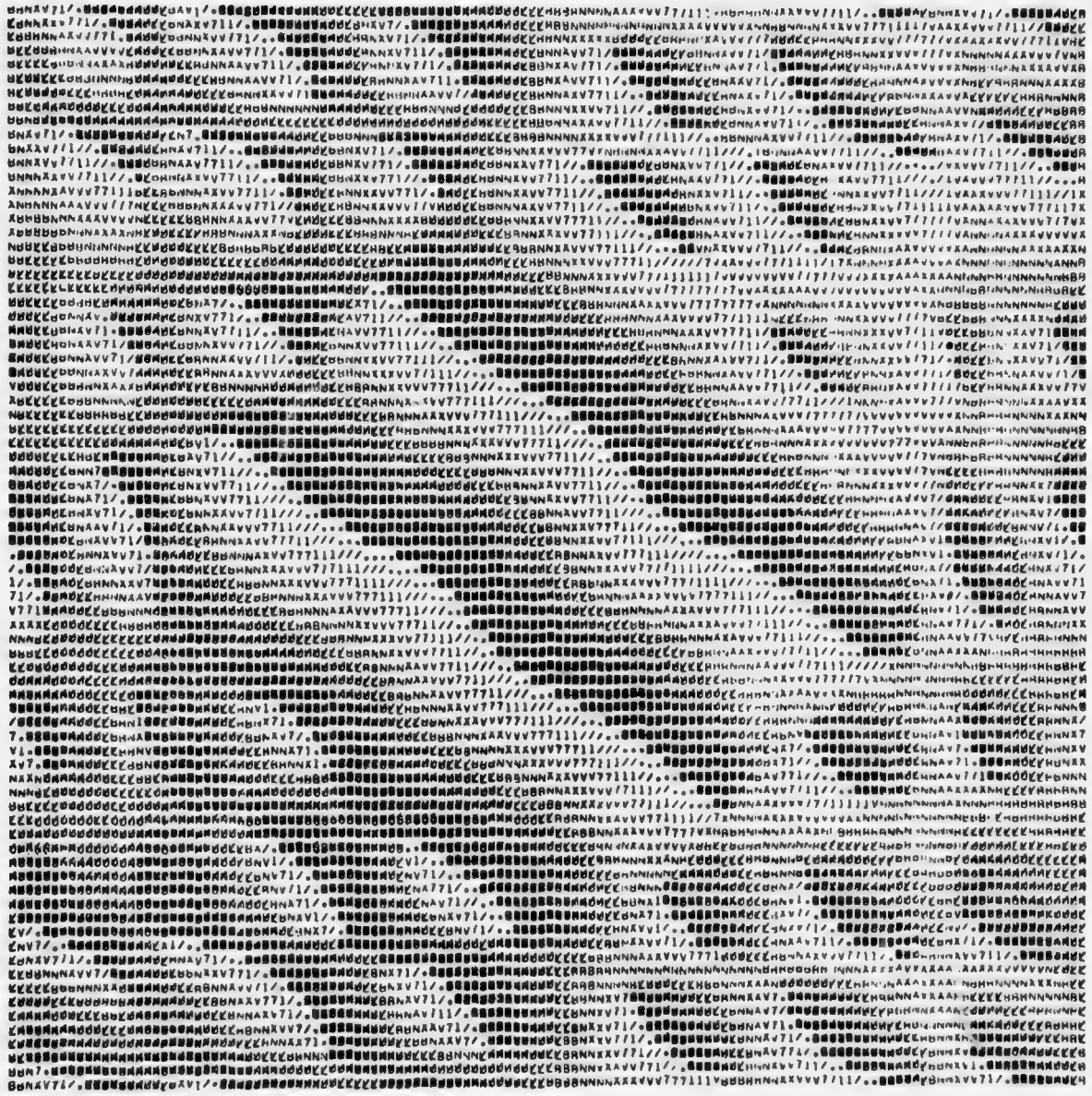

Figure 12. Phase Response of Filter 2.1.

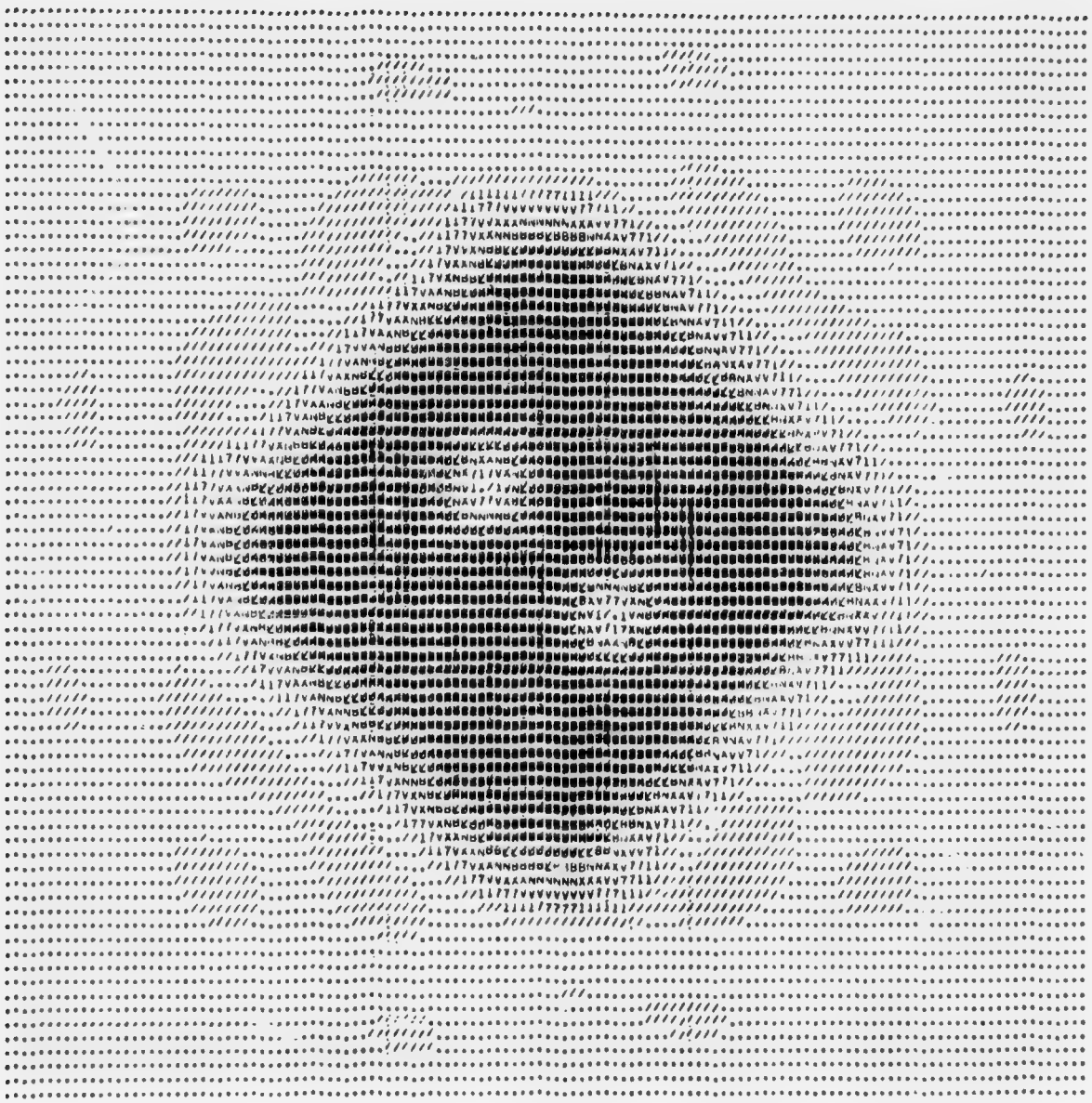

Figure 13. Amplitude Response of Filter 2.2.

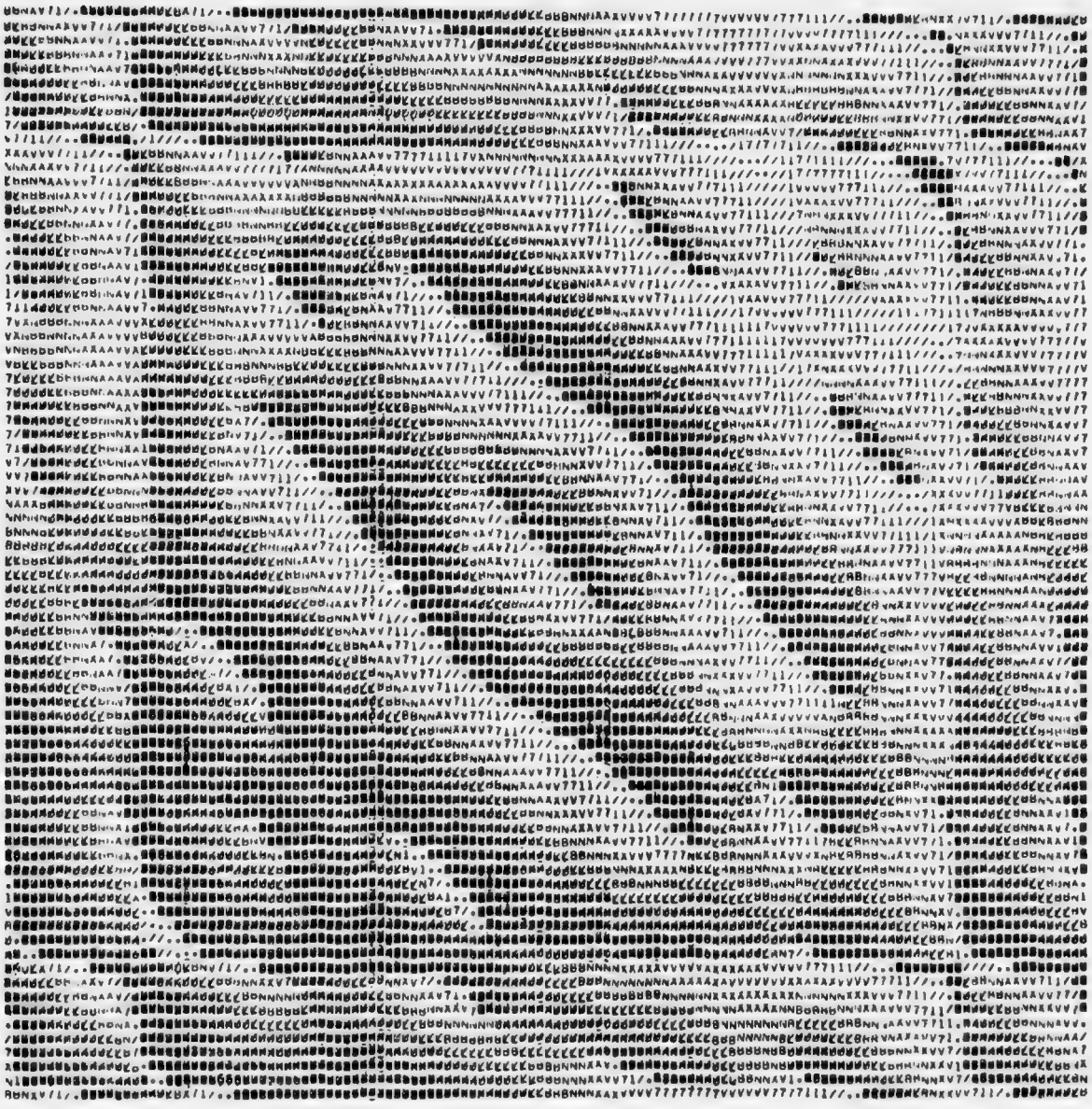

Figure 14. Phase Response of Filter 2.2.

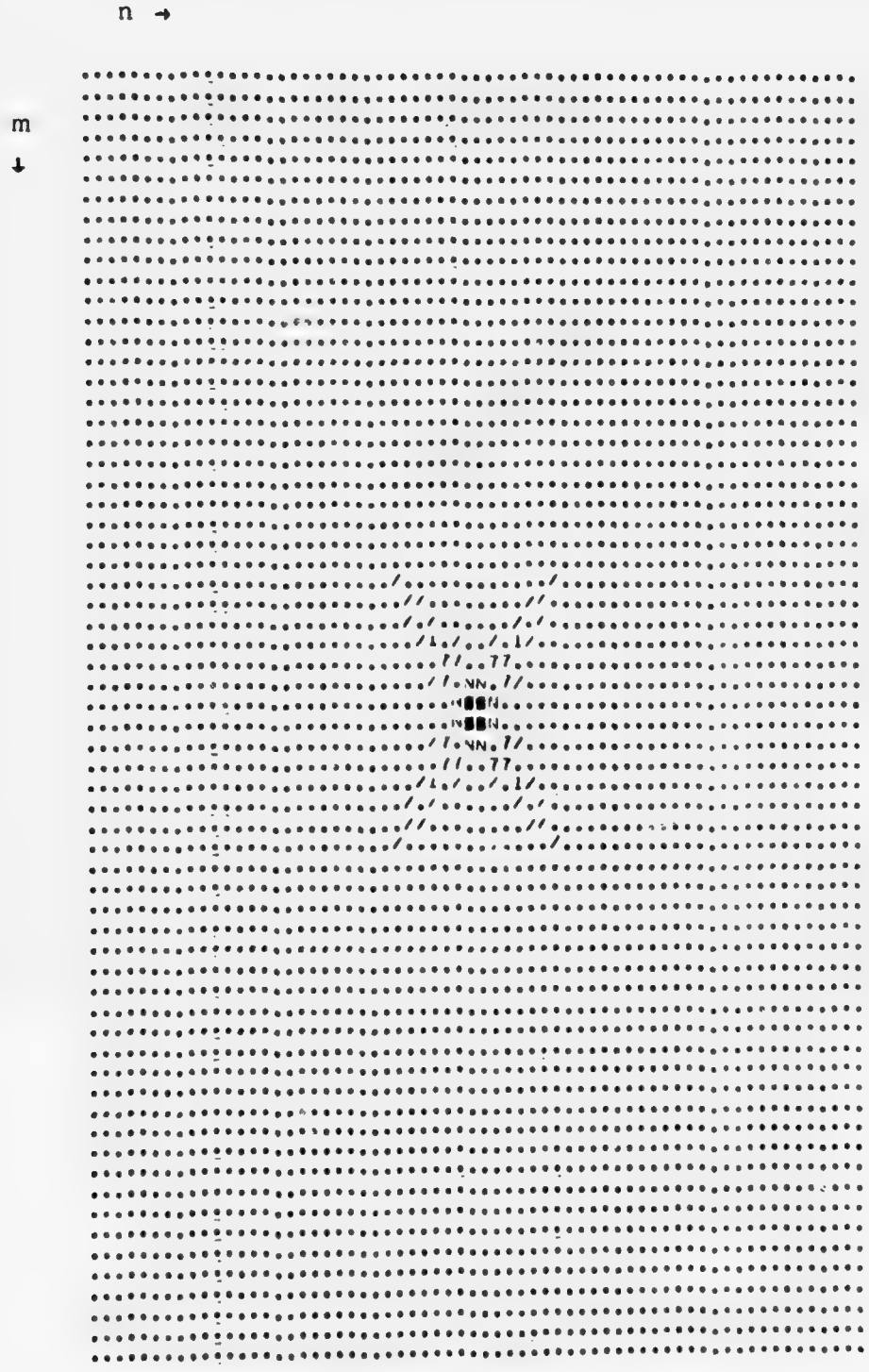

Figure 15. $\{|\tilde{h}^{0}_{mn}|\}$ For Filter 2.2.

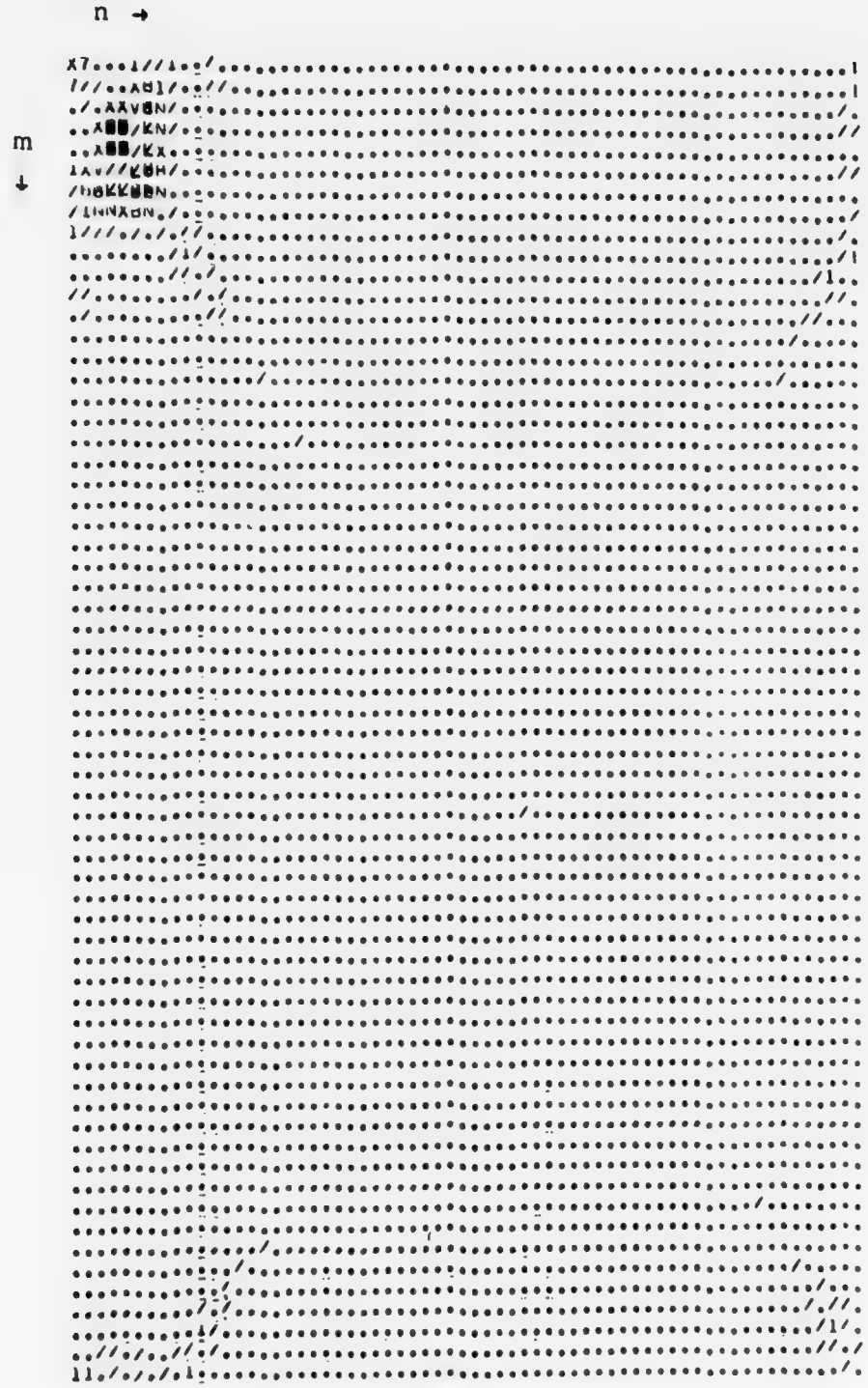

Figure 16. $\{|\tilde{h}^{99}_{mn}|\}$ For Filter 2.2.

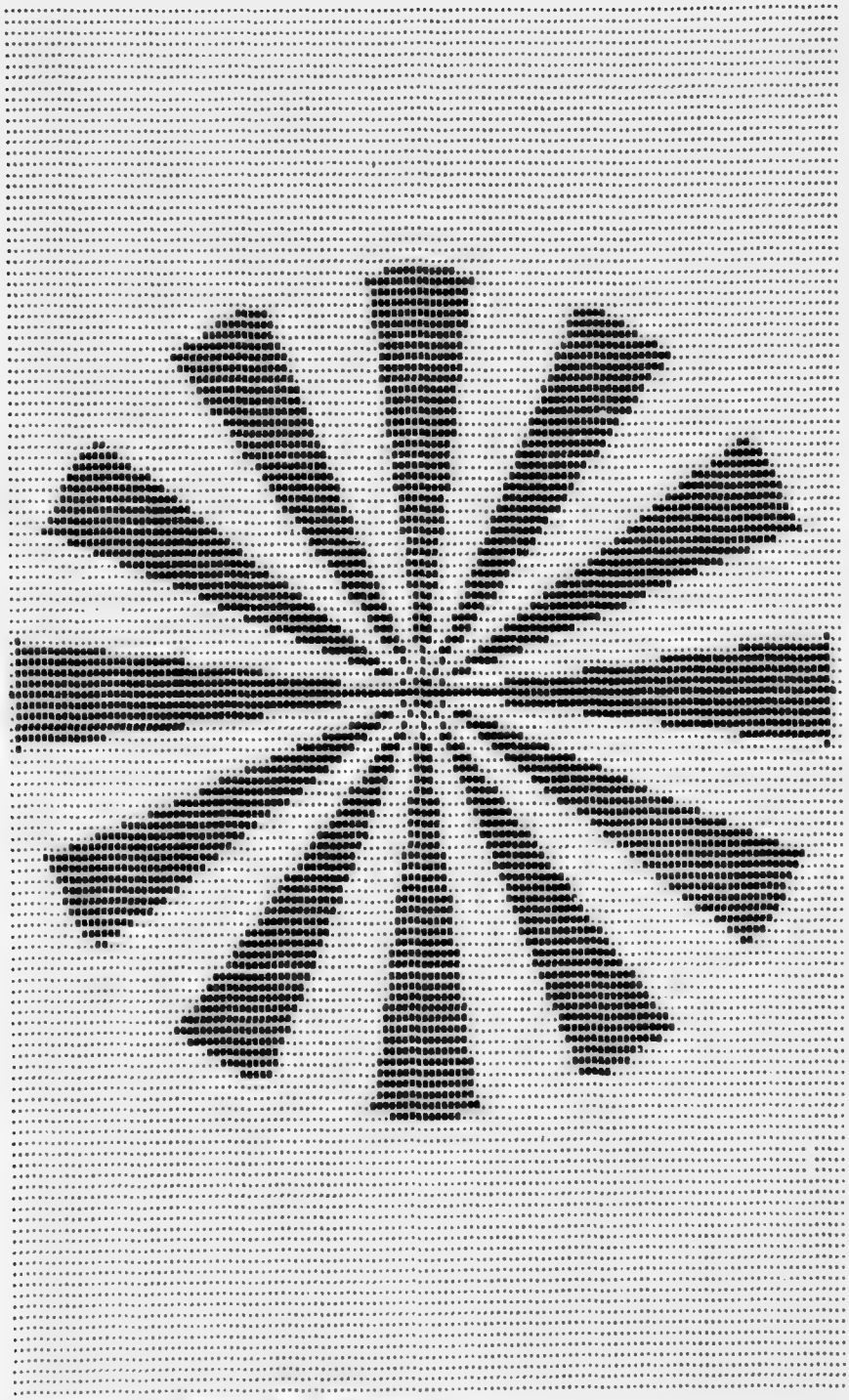

Figure 17, Spoke Test Pattern

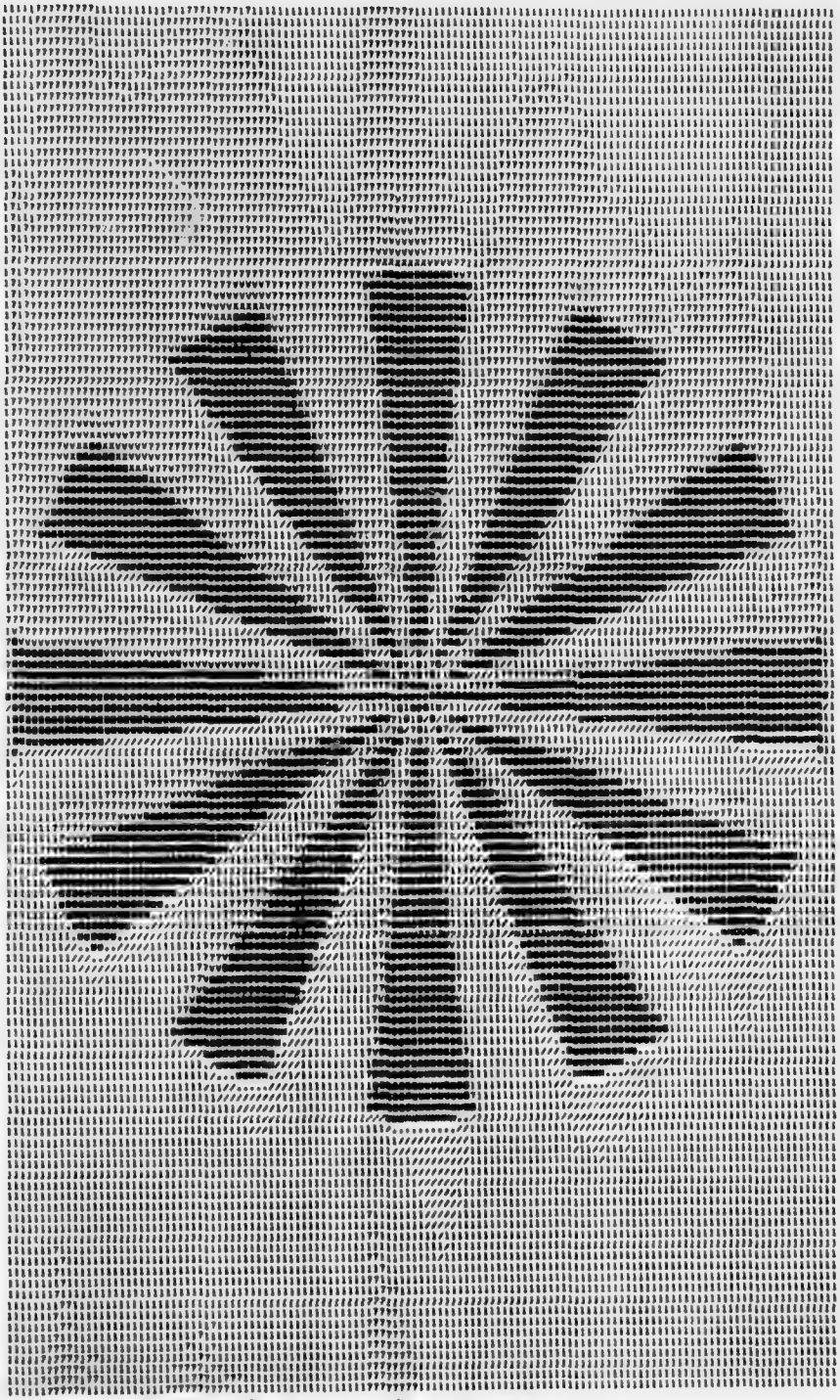

Figure 18. $\{\hat{p}_{mn}\}$ for $D(p,\hat{p}) = .0096$

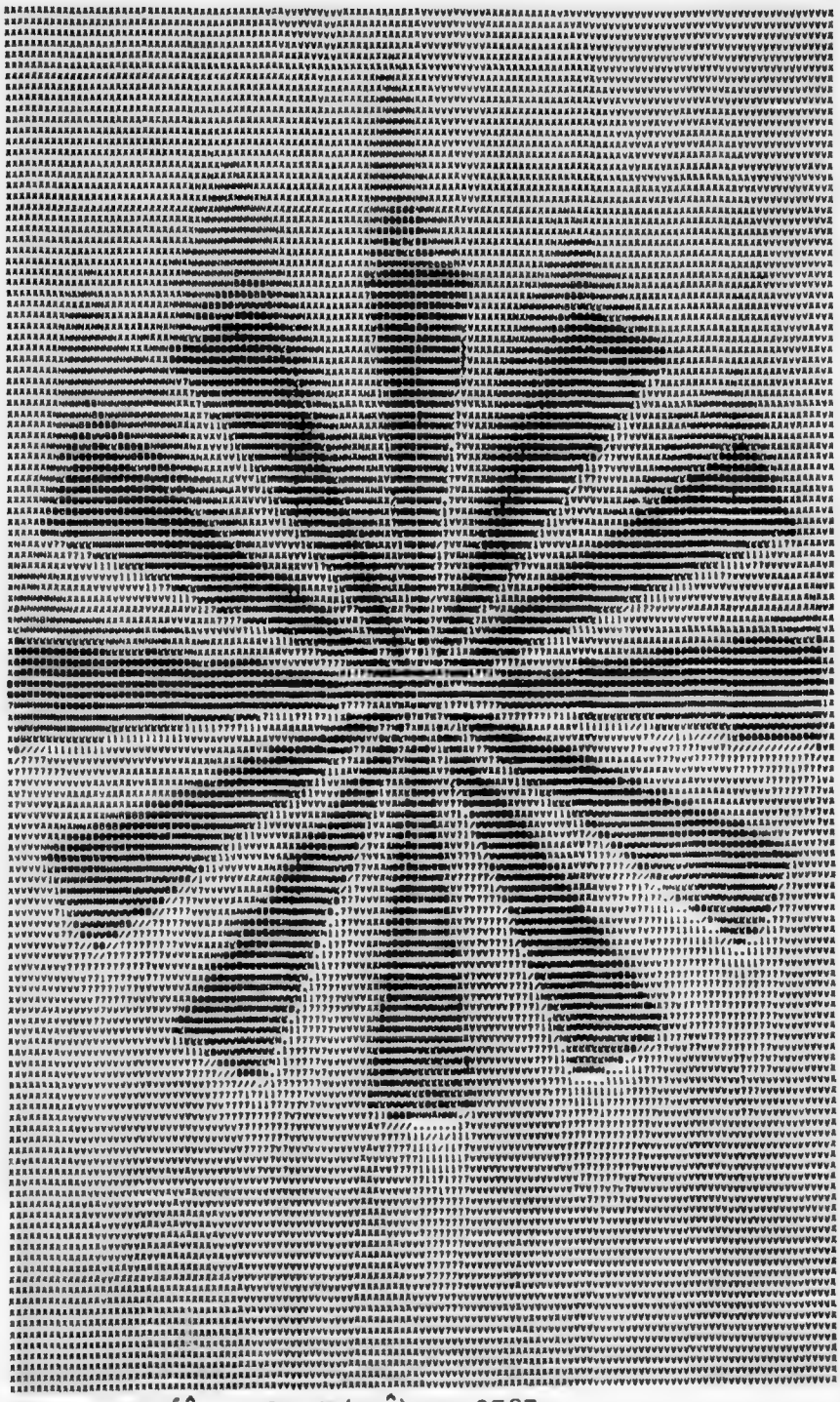

Figure 19. $\{\hat{p}_{mn}\}$ for $D(p,\hat{p}) = .0787$

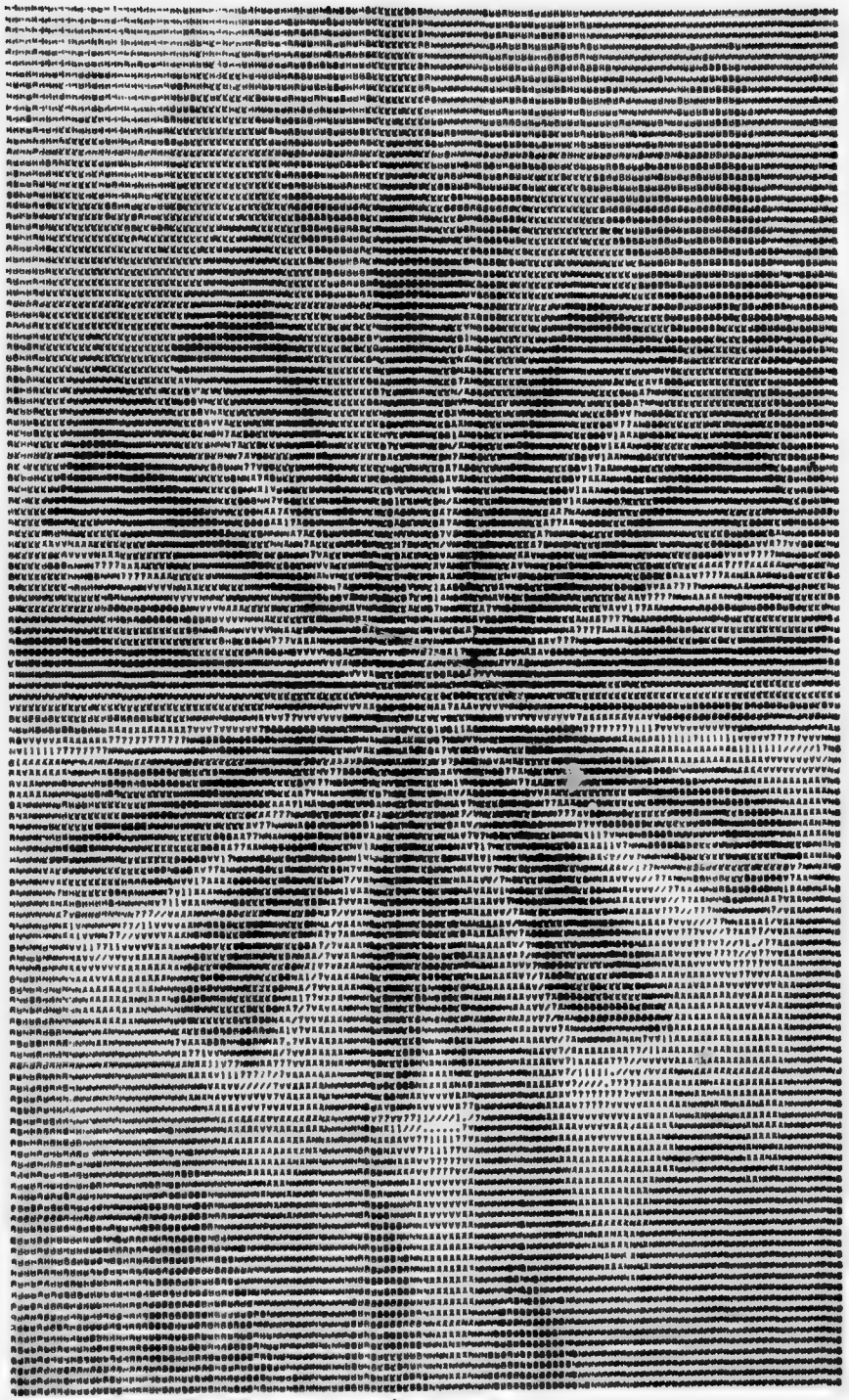

Figure 20. $\{\hat{p}_{mn}\}$ for $D(p,\hat{p}) = .32$

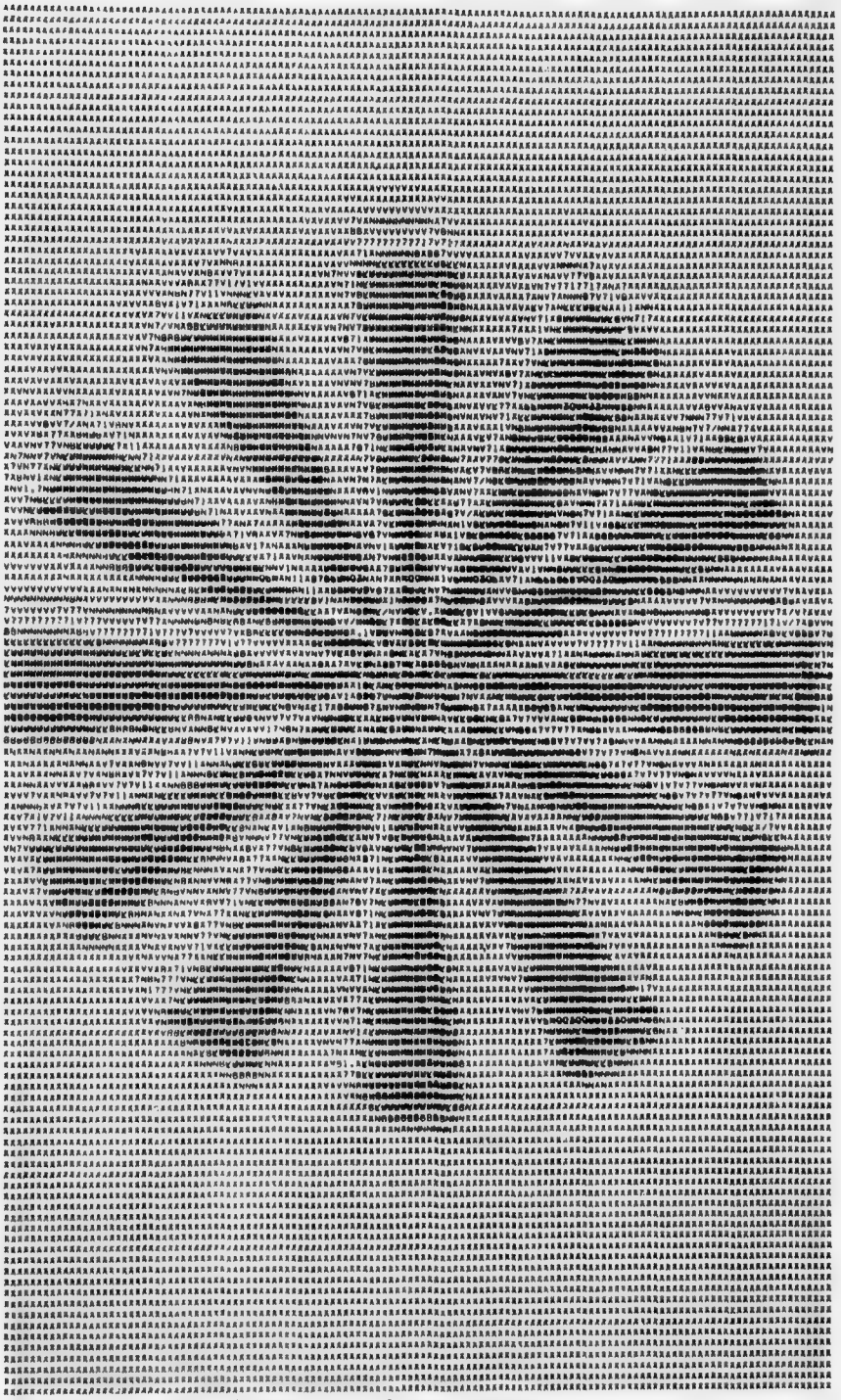

Figure 21. $\{\hat{p}_{mn}\}$ for $D(p,\hat{p}) = .0779$

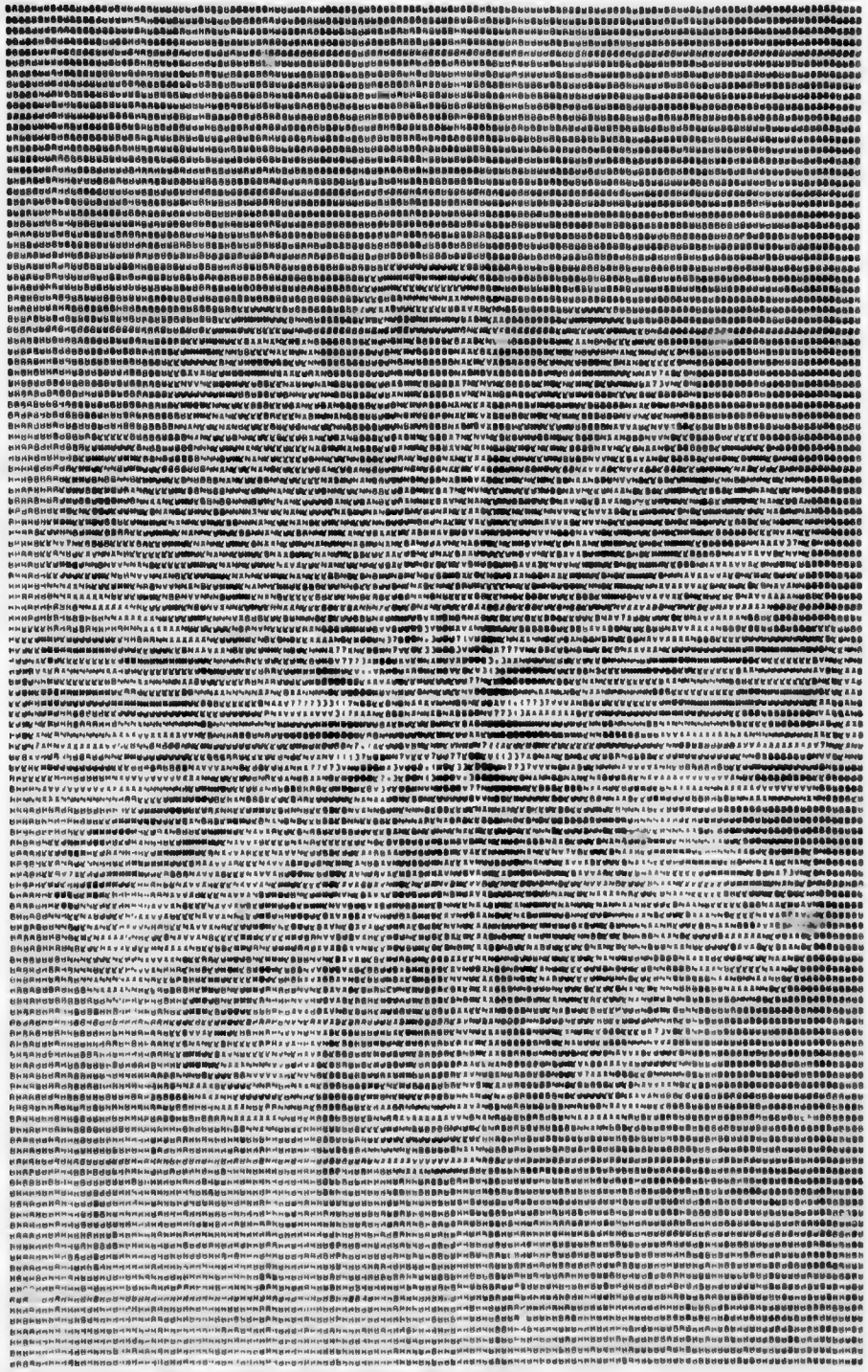

Figure 22. Output Picture for Filter 1.2

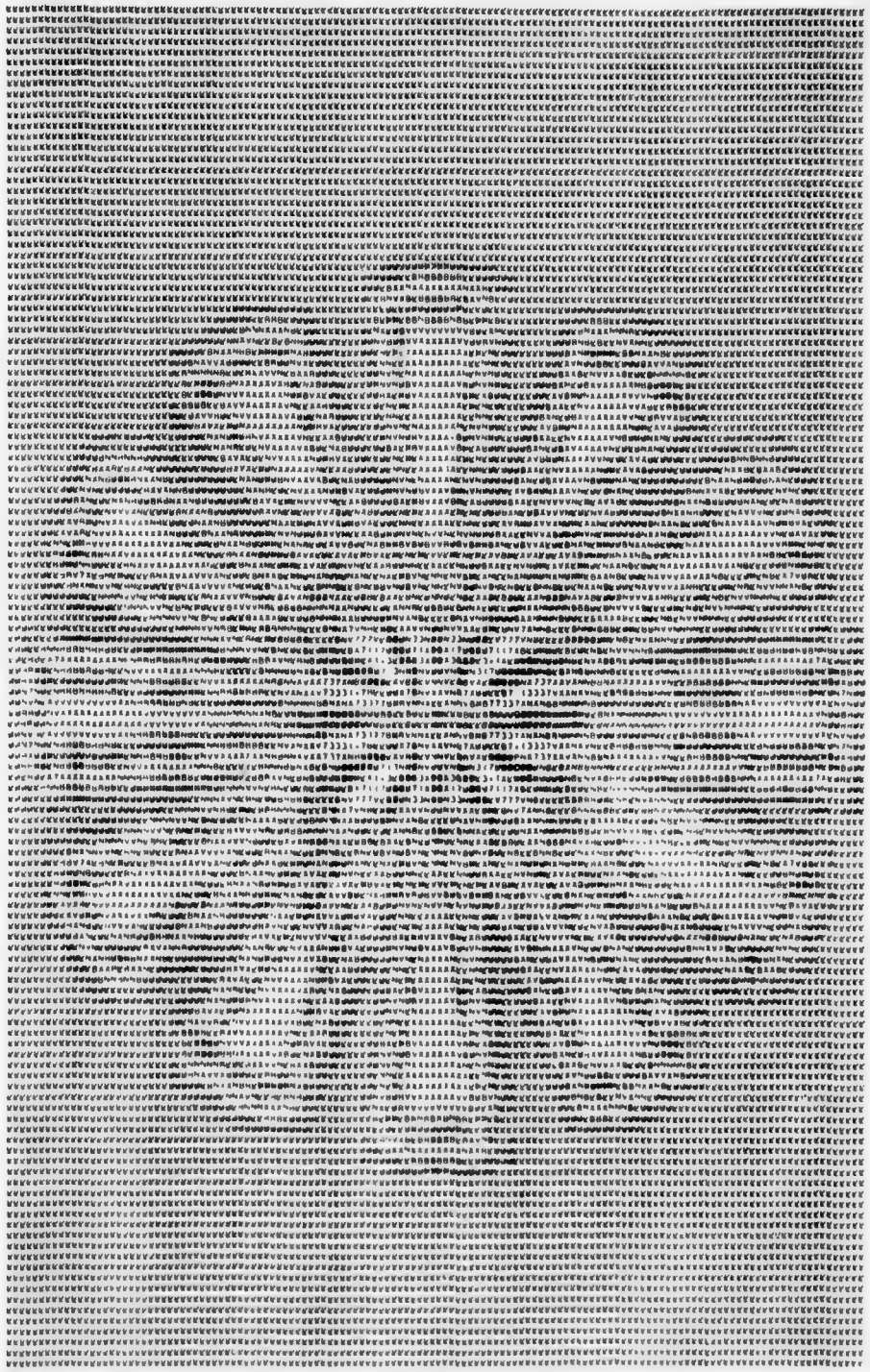

Figure 23. Output Picture for Filter 1.3

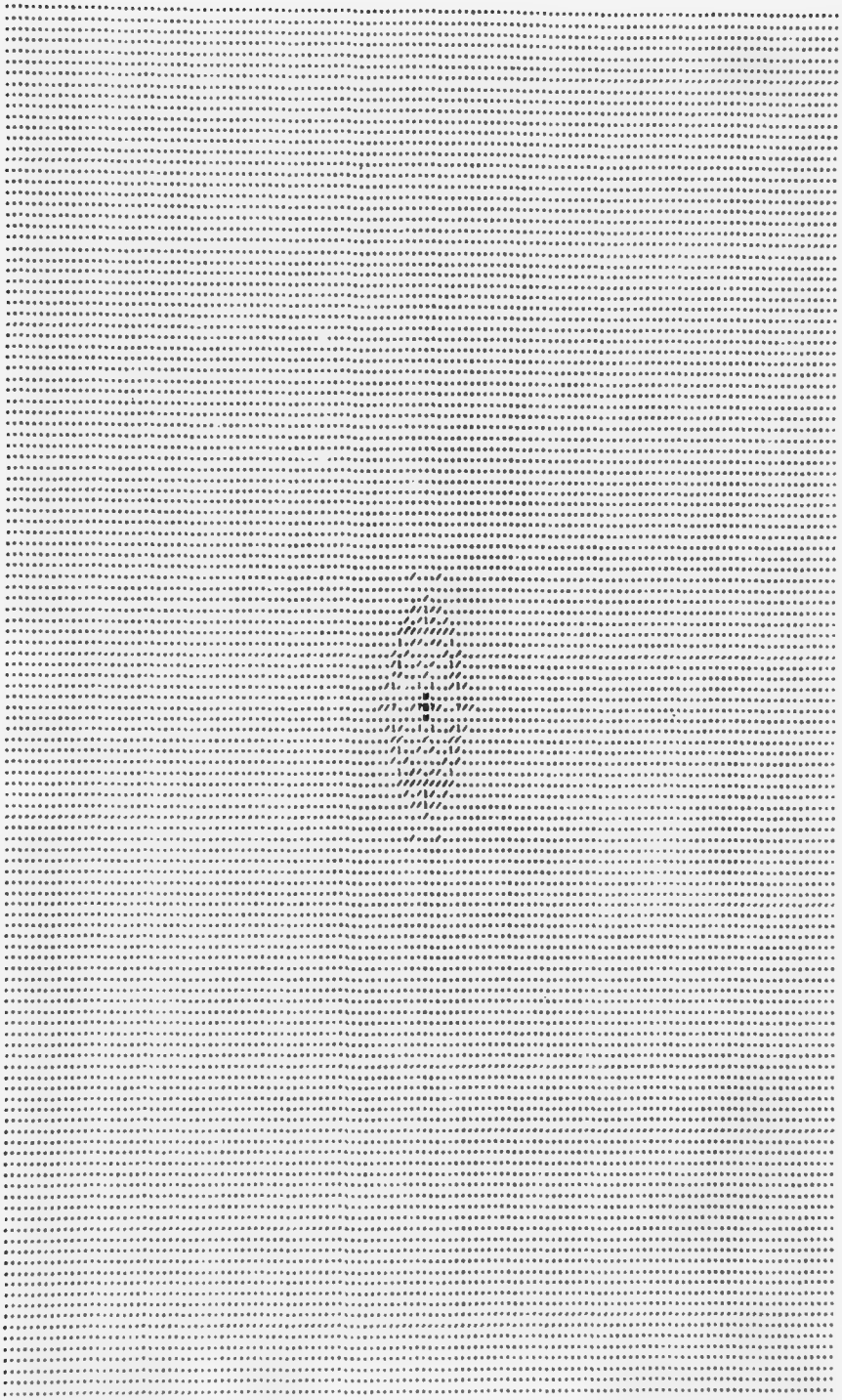

Figure 24. $\{|F_{k\ell}|\}$

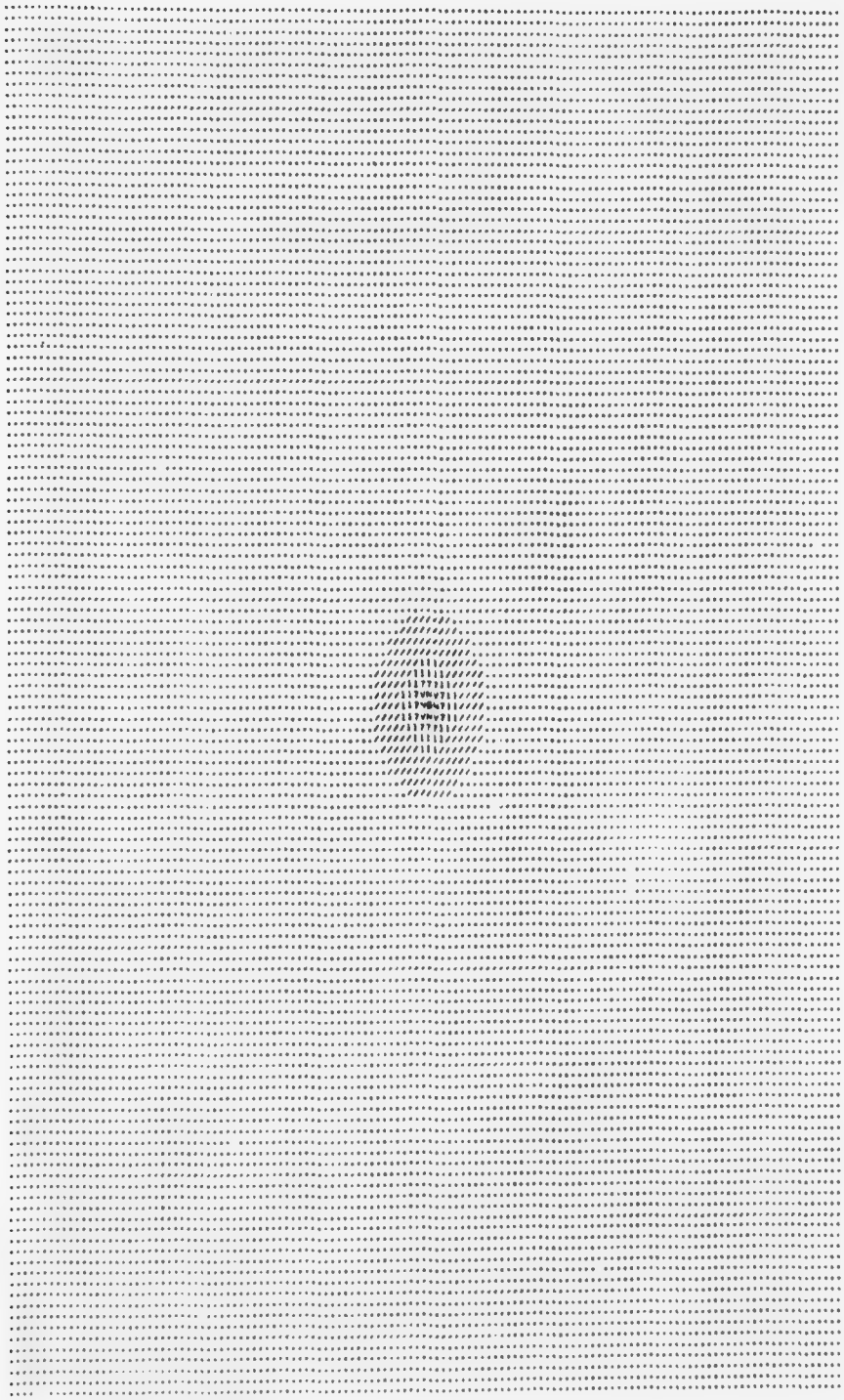

Figure 25. $\{|\tilde{F}_{k\ell}|\}$

m \ n							
-.018013	.011921	.035469	.038566	.038510	.037816	.037457	.018353
.011921	.048624	.032796	-.011562	-.023343	-.000627	.028085	.041197
.035469	.032796	-.047551	-.099203	-.081825	-.063714	-.046704	-.005947
.038566	-.011562	-.099203	-.062272	.039716	.016653	-.072099	-.061767
.038510	-.023343	-.081825	.039716	.205493	.148226	-.028614	-.064013
.037816	-.000627	-.063714	.016653	.148226	.113237	-.018027	-.039705
.037457	.028085	-.046704	-.072099	-.028614	-.018027	-.031938	-.009887
.018353	.041197	-.005947	-.061767	-.064013	-.039705	-.009887	.015989

Table 1. Coefficients of Filter 1.1.

m \ n							
-.010296	-.012174	-.004607	.018332	.046726	.055816	.042038	.020415
-.012174	.010842	.032996	.026270	.005043	-.001162	.018423	.036120
-.004607	.032996	.025879	-.025790	-.03639	-.111444	-.077537	-.009811
.018332	.026270	-.025790	-.048502	-.027237	-.042142	-.069416	-.037426
.046726	.005043	-.083639	-.027237	.134393	.154105	.030343	-.024571
.055816	-.001162	-.111444	-.042142	.154105	.180039	.028599	-.042062
.042038	.018423	-.077537	-.069416	.030343	.028599	-.057042	-.064178
.020415	.036120	-.009811	-.037426	-.024571	-.042062	-.064178	-.019642

Table 2. Coefficients of Filter 1.2.

	n							
m	.011371	.025437	.010680	-.002393	-.001537	.011293	.025164	.012355
	.025437	-.002390	-.055940	-.071665	-.073245	-.055734	-.002765	.025164
	.010680	-.055940	-.063769	-.002361	-.000140	-.064456	-.055734	.011293
	-.002393	-.071665	-.002361	.173137	.169481	-.000140	-.073245	-.001537
	-.001537	-.073245	-.000140	.169481	.173137	-.002361	-.071665	-.002393
	.011293	-.055734	-.064456	-.000140	-.002361	-.063769	-.055940	.010680
	.025164	-.002765	-.055734	-.073245	-.071665	-.055940	-.002390	.025437
	.012355	.025164	.011293	-.001537	-.002393	.010680	.025437	.011371

Table 3. Coefficients of Filter 1.3.

m \ n							
.025139	.004439	.002426	.012435	.005909	.010801	.037184	.036031
.000938	-.028609	-.017440	.005531	-.007500	-.013174	.020517	.037184
-.032758	-.048371	-.000712	.044408	.013378	-.028987	-.013174	.010801
-.022710	-.005583	.088968	.157988	.104458	.013378	-.007500	.005909
-.007292	.026004	.142080	.221729	.157988	.044408	.005531	.012435
-.032276	-.020083	.072936	.142080	.088968	-.000712	-.017440	.002426
-.046795	-.067664	-.020083	.026004	-.005583	-.048371	-.028609	.004439
-.015733	-.046795	-.032276	-.007292	-.022710	-.032758	.000938	.025139

Table 4. Coefficients of Filter 2.1.

m \ n							
.043750	.031571	.000991	-.002615	-.002387	-.020250	-.015530	.013693
.031571	.010139	-.012724	-.000236	-.003619	-.047863	-.059947	-.017666
.000991	-.012724	-.003251	.044381	.041672	-.040269	-.089892	-.053981
-.002615	-.000236	.044381	.126073	.126847	.014375	-.071270	- -.051563
-.002387	-.003619	.041672	.126847	.129431	.016134	-.069340	-.046307
-.020250	-.047863	-.040269	.014375	.016134	-.066415	-.112419	-.063547
-.015530	-.059947	-.089892	-.071270	-.069340	-.112419	-.116071	-.052429
.013693	-.017666	-.053981	-.051563	-.046307	-.063547	-.052429	-.006065

Table 5. Coefficients of Filter 2.2.

BIBLIOGRAPHY

[1] T. C. Rindfleisch, J. A. Dunne, H. J. Frieden, W. D. Stromberg, and R. M. Ruiz, "Digital Processing of the Mariner 6 and 7 Pictures," Journal of Geophysics Research, vol. 76, pp. 394-417, January 1971.

[2] T. G. Stockham, Jr., T. M. Cannon, and R. B. Ingebretsen, "Blind Deconvolution Through Digital Signal Processing," Proceedings of the IEEE, pp. 678-692, April 1975.

[3] B. L. Lewis and D. J. Sakrison, "Computer Enhancement of Scanning Electron Micrographs," IEEE Transactions on Circuits and Systems, vol. CAS-22, pp. 267-278, March 1975.

[4] R. O. Duda and P. E. Hart. Pattern Classification and Scene Analysis, John Wiley and Sons, New York, 1973.

[5] H. S. Hersey and R. M. Mersereau, "An Algorithm to Perform Minimax Approximation in the Absence of the Haar Condition," Quarterly Progress Report No. 114, M.I.T., Res. Lab. of Elec., pp. 160-171, July 15, 1974.

[6] J. V. Hu and L. R. Rabiner, "Design Techniques for Two-Dimensional Digital Filters," IEEE Transactions on Audio and Electroacoustics, vol. AU-20, pp. 249-257, Oct. 1972.

[7] J. H. McClellan, "The Design of Two-Dimensional Digital Filters by Transformations," Proceedings of the Seventh Annual Princeton Conference on Information Sciences and Systems, pp. 247-251, March 1973.

[8] T. S. Huang, "Two Dimensional Windows," IEEE Transactions on Audio and Electroacoustics, vol. AU-20, no. 1, pp. 88-89, March 1972.

[9] Lewis Larmore, H. M. A. El-Sum, and A. F. Metherell, "Acoustical Holograms Using Phase Information Only," Applied Optics, vol. 8, no. 8, pp. 1533-1536, August 1969.

[10] Dorian Kermisch, "Image Reconstruction From Phase Information Only," JOSA, vol. 60, no. 1, pp. 15-17, January 1970.

[11] T. S. Huang, J. W. Burnett, and A. G. Deczky, "The Importance of Phase in Image Processing Filters," IEEE Transactions on Acoustics, Speech, and Signal Processing, vol. ASSP-23, no. 6, pp. 529-542, December 1975.

[12] K. Steiglitz, "Computer-Aided Design of Recursive Digital Filters," IEEE Transactions on Audio and Electroacoustics, vol. AU-18, no. 2, pp. 123-129, June 1970.

[13] C. Goffman, Introduction to Real Analysis, Harper and Row, Publishers, New York, 1966.

[14] D. J. Wilde and C. S. Beightler, Foundations of Optimization, Prentice-Hall, Inc., Englewood Cliffs, N. J., 1967.

[15] J. W. Goodman, Introduction to Fourier Optics, McGraw-Hill Book Company, New York, 1968.

UNCLASSIFIED

SECURITY CLASSIFICATION OF THIS PAGE (When Data Entered)

REPORT DOCUMENTATION PAGE		READ INSTRUCTIONS BEFORE COMPLETING FORM
1. REPORT NUMBER AFOSR - TR - 77 - 0008	2. GOVT ACCESSION NO.	3. RECIPIENT'S CATALOG NUMBER
4. TITLE (and Subtitle) THE DESIGN OF MULTIDIMENSIONAL FIR DIGITAL FILTERS BY PHASE CORRECTION		5. TYPE OF REPORT & PERIOD COVERED INTERIM 6. PERFORMING ORG. REPORT NUMBER
7. AUTHOR(s) J. K. Aggarwal M. T. Manry		8. CONTRACT OR GRANT NUMBER(s) Cont. F44620-76-C-0089
9. PERFORMING ORGANIZATION NAME AND ADDRESS Electronics Research Center The University of Texas at Austin Austin, Texas 78712		10. PROGRAM ELEMENT, PROJECT, TASK AREA & WORK UNIT NUMBERS 4751 61102F 681306
11. CONTROLLING OFFICE NAME AND ADDRESS AF Office of Scientific Research (NE) Bolling AFB DC 20332		12. REPORT DATE August 12, 1976 13. NUMBER OF PAGES 85
14. MONITORING AGENCY NAME & ADDRESS(if different from Controlling Office)		15. SECURITY CLASS. (of this report) UNCLASSIFIED 15a. DECLASSIFICATION/DOWNGRADING SCHEDULE

16. DISTRIBUTION STATEMENT (of this Report)

Approved for public release; distribution unlimited.

17. DISTRIBUTION STATEMENT (of the abstract entered in Block 20, if different from Report)

18. SUPPLEMENTARY NOTES

19. KEY WORDS (Continue on reverse side if necessary and identify by block number)

MULTIDIMENSIONAL FIR DIGITAL FILTERS
PICTURE PROCESSING
TWO-DIMENSIONAL PHASE
PHASE DISTORTION

20. ABSTRACT (Continue on reverse side if necessary and identify by block number)

This report presents a new technique for the design of multidimensional FIR digital filters. Given the desired amplitude response, the truncation error or a low order approximation to a high order filter is iteratively decreased by varying the phase response. Convergence of the iterative algorithm is discussed. In general, the phase responses of the filters resulting from the algorithm are nonlinear. Pictures suffer phase distortion when filters with nonlinear phase characteristics are used in filtering. A measure of phase

(continued)

DD FORM 1 JAN 73 1473 EDITION OF 1 NOV 65 IS OBSOLETE

UNCLASSIFIED

SECURITY CLASSIFICATION OF THIS PAGE (When Data Entered)

distortion in pictures is introduced so that the effects of nonlinear phase in filters may be quantified. Examples illustrating the use of the design technique and the measure of phase distortion are included. The results of this report are formulated in two dimensions; however they are valid for filters and signals of any dimension.